FINAL PROJECT REPORT # 00055304

GRANT: DTRT13-G-UTC45
Project Period: 6/1/2016 – 12/31/19

Volume II: Investigation On Thixotropy Of Vibration-Free Concrete Mixtures Intended For Rapid Pavement Construction

Participating Consortium Member:
Missouri University of Science and Technology

Authors:
Dimitri Feys, Assistant Professor
Piyush Rajendra Lunkad, Graduate Assistant
Missouri University of Science and Technology

RE-CAST:
REsearch on Concrete Applications for Sustainable Transportation
Tier 1 University Transportation Center

DISCLAIMER

The contents of this report reflect the views of the authors, who are responsible for the facts and the accuracy of the information presented herein. This document is disseminated under the sponsorship of the U.S. Department of Transportation's University Transportation Centers Program, in the interest of information exchange. The U.S. Government assumes no liability for the contents or use thereof.

TECHNICAL REPORT DOCUMENTATION PAGE

1. Report No. RECAST UTC #00055304	**2. Government Accession No.**	**3. Recipient's Catalog No.**
4. Title and Subtitle Volume II: Investigation On Thixotropy Of Vibration-Free Concrete Mixtures Intended For Rapid Pavement Construction		**5. Report Date** January 2020 **6. Performing Organization Code:**
7. Author(s) Dimitri Feys and Piyush Rajendra Lunkad		**8. Performing Organization Report No.** Project #00055304
9. Performing Organization Name and Address RE-CAST – Missouri University of Science and Technology 500 W. 16th St., 223 ERL Rolla, MO 65409-0710		**10. Work Unit No.** **11. Contract or Grant No.** USDOT: DTRT13-G-UTC45
12. Sponsoring Agency Name and Address Office of the Assistant Secretary for Research and Technology U.S. Department of Transportation 1200 New Jersey Avenue, SE Washington, DC 20590		**13. Type of Report and Period Covered:** Final Report Period: 6/1/2016 – 12/31/19 **14. Sponsoring Agency Code:**
15. Supplementary Notes The investigation was conducted in cooperation with the U. S. Department of Transportation.		

16. Abstract

This report discusses the advances and setbacks encountered when attempting to develop a vibration-free, self-consolidating concrete for slipform applications. Such concrete would have significant advantages compared to conventional slipforming, as vibration would not be necessary. All negative aspects of incorrect vibration, such as inadequate air content (too much entrapped air or insufficient entrained air), and segregation, which on its turn could lead to inferior freeze-thaw and scaling resistance or cracking, would be avoided [1] [2] [3] [4]. Based on previous work [5] [6], further referenced in the literature review, the research team wanted to attain a higher slump flow (> 550 mm) to ensure full self-consolidation, while also showing substantial thixotropy to develop the necessary shape stability.

Current techniques in the development of 3D printing, which require similar properties of the construction material, use different chemical admixtures added at specific times when necessary. As an example, some mixtures are heavily retarded, and a large amount of accelerator is added just before the material passes through the nozzle [7] [8]. Although this technique would be certainly applicable for slipforming, it is questionable whether this can be executed on a large scale such as slipforming. Any mistakes in timing or dosage of the admixtures, or inadequate incorporation or distribution of the admixtures in the concrete would result in disastrous increases in cost as the concrete would remain too fluid or harden too soon, dependent on the error. As such, the team has chosen to pursue an approach in which intervening on the jobsite would be kept to a minimum in order to avoid those errors.

In this report, a literature review is made on previous work on this topic, as well as a revision of how constituent materials influence thixotropy. Some basic concepts from physics and chemistry are also highlighted as they are applicable to this work. The material properties, mix designs and testing protocols are described in section 3, while the results for cement paste and concrete are discussed in sections 4 and 5, respectively. Section 6 concludes this report.

17. Key Words vibration-free, self-consolidating concrete	**18. Distribution Statement** No restrictions. This document is available to the public.	
19. Security Classification (of this report) Unclassified	**20. Security Classification (of this page)** Unclassified	**21. No of Pages** 67

Table of Contents

List of Figures

List of Tables

1 Introduction

This report discusses the advances and setbacks encountered when attempting to develop a vibration-free, self-consolidating concrete for slipform applications. Such concrete would have significant advantages compared to conventional slipforming, as vibration would not be necessary. All negative aspects of incorrect vibration, such as inadequate air content (too much entrapped air or insufficient entrained air), and segregation, which on its turn could lead to inferior freeze-thaw and scaling resistance or cracking, would be avoided [1] [2] [3] [4]. Based on previous work [5] [6], further referenced in the literature review, the research team wanted to attain a higher slump flow (> 550 mm) to ensure full self-consolidation, while also showing substantial thixotropy to develop the necessary shape stability.

Current techniques in the development of 3D printing, which require similar properties of the construction material, use different chemical admixtures added at specific times when necessary. As an example, some mixtures are heavily retarded, and a large amount of accelerator is added just before the material passes through the nozzle [7] [8]. Although this technique would be certainly applicable for slipforming, it is questionable whether this can be executed on a large scale such as slipforming. Any mistakes in timing or dosage of the admixtures, or inadequate incorporation or distribution of the admixtures in the concrete would result in disastrous increases in cost as the concrete would remain too fluid or harden too soon, dependent on the error. As such, the team has chosen to pursue an approach in which intervening on the jobsite would be kept to a minimum in order to avoid those errors.

In this report, a literature review is made on previous work on this topic, as well as a revision of how constituent materials influence thixotropy. Some basic concepts from physics and chemistry are also highlighted as they are applicable to this work. The material properties, mix designs and testing protocols are described in section 3, while the results for cement paste and concrete are discussed in sections 4 and 5, respectively. Section 6 concludes this report.

2 Literature Review

2.1 What is Vibration-Free Concrete for Slipforming?

The first concept for vibration-free concrete (VFC) for slipforming stems from the benefits of self-consolidating concrete (SCC) in the construction industry. SCC has excellent flowability, passing ability and stability [9]. It typically also increases surface quality [10], reduces energy consumption, vibration and noise pollution caused by standard concrete operations. Such concrete has been applied for slipforming, but a reduction in fluidity was imposed. While typical slump flow values for regular SCC vary between roughly 600 and 800 mm, the SCC for slipforming has a recommended slump flow value between 325 and 375 mm [11]. It is stated in [11] that this concrete has the ability to self-consolidate and to hold its own shape with minimal consolidation energy. In fact, the high fluidity and shape stability requirements are contradictory and require rapid development of stiffness and green strength once the material no longer flows [5].

In a feasibility study for VFC for slipforming [5], the rheological response of mixtures with various fine minerals (e.g. nano-clays), supplementary cementitious materials (SCMs) or chemical admixtures was studied to evaluate the workability and green strength development of VFC for slipforming. It has been observed that rheological properties play a significant role in the follow-up study for the selection of materials, the mix proportioning and understanding the flowability and green strength of VFC for slipforming [6]. In addition, to further validate the performance of the developed VFC for slipforming, hardened properties should be comparable to those of conventional slip form pavement concrete in terms of strength, durability, and sustainability. The results indicated that properties such as heat of hydration, porosity, rapid chloride ion permeability and freeze-thaw durability were comparable to those of conventional concrete, while properties such as compressive strength and shrinkage were more elevated than for conventional concrete [6]. The field implementation conducted by Wang et al. [6] shows that VFC for slipforming can be prepared in a batching plant. Wang et al. [6] proposed that modifications in the paver machine during the placement and extrusion process are required for the proper distribution of the VFC along the width, and a horizontal leg to mold and hold the fresh concrete mixture for a sufficiently long duration until it has developed adequate green strength. The field implementation study also shows on-site modifications of water and high-range water reducer (HRWR) agent to achieve target workability. This may be necessary to reduce a loss of workability with transport time and to mitigate the influence of other added rheology-modifying agents.

Based on the above studies, it is clear that VFC for slipforming is feasible. However, the proposed fluidity levels are relatively low and other research has shown that such concrete will need some consolidation to remove entrapped air, especially if the viscosity would be more elevated [12]. As mentioned previously, the fluidity and shape stability requirements are contradictory. The research team intended to find a strategy to simultaneously satisfy those requirements, based on concepts of paste and concrete rheology. The remaining part of the literature review concentrates on some principles of rheology, measuring techniques, and the influence of constituent elements on desired rheological properties.

2.2 Rheological Properties of Cement-Based Materials

Rheology is defined as the science of deformation of matter [13]. Typically, a distinction is made between solids and liquids, with visco-elastic materials being an intermediate class, as their response is dependent on the magnitude and duration of the stress or strain. In the first hours after contact between cement and water, cement-based materials can be considered as a liquid suspension with a high amount of particles. At least, this is the case if the concentration of aggregate does not exceed a critical value causing friction [14]. In this suspension, the rheological properties vary with time due to the physical process of flocculation and the

chemical process of cement hydration [15] [16] [17]. In the following sections, rheological properties and corresponding measurements are described as a function of the time scale of observation.

2.2.1 Steady-state rheological properties

If the rheological properties are determined on a relatively short time-scale, during which we can assume they do not change, steady-state properties are obtained. Considering the material as a liquid, the relationship between the shear stress and shear rate (= velocity gradient) must be characterized. In a majority of the cases, the shear stress – shear rate curve is linear, but it intersects the stress axis at a non-zero stress value [18] [19]. This latter stress value is named the yield stress: for a shear stress below the yield stress, the shear rate is zero [18] [20]. The material will undergo an elastic strain but will not flow. Once the yield stress is exceeded, the material flows. The slope of the line defines how much the flow will be accelerated by an increase in shear stress. This slope is called the differential viscosity (not to be confused with apparent viscosity). High viscosity materials require a large stress increase for a certain increase in shear rate, while low viscosity materials require a lower increase in stress to obtain the same increase in shear rate [13] [18].

The Bingham model (Eq. 1) describes the behavior discussed in the paragraph above. It shows that the shear stress (τ) equals the sum of the yield stress (τ_0) and the product of the viscosity (μ_p) multiplied by the shear rate ($\dot{\gamma}$). In the Bingham model, this (differential) viscosity is also called the plastic viscosity.

$$\tau = \tau_0 + \mu_p \dot{\gamma} \qquad \textit{(Eq. 1)}$$

In some exceptional cases, the material behaves non-linearly: the relationship between shear stress and shear rate either curves up or down. In the former case, the slope of the curve increases with increasing shear rate and the material displays shear-thickening behavior [21] [22]. In the latter case, the slope of the curve decreases with increasing shear rate and the material is shear-thinning [23]. In both cases, the Bingham model is not valid, and an alternative model must be selected. Many models are available to fit the data, among which are the Herschel-Bulkley and the modified Bingham model [23]. For this research work, the modified Bingham model (Eq. 2) had to be employed on certain mixtures due to non-negligible shear-thickening.

$$\tau = \tau_0 + \mu_p \dot{\gamma} + c\dot{\gamma}^2 \qquad \textit{(Eq. 2)}$$

2.2.2 Time-dependent rheological properties

Extending the time scale of observation beyond a couple of minutes will induce some changes in the rheological properties of the material. These changes are caused by two separate phenomena: flocculation and hydration. Flocculation is the consequence of inter-particle forces on a sub-micron level [20]. The balance between Van der Waals attraction forces and electrostatic repulsion or steric hindrance causes an energy potential around each small particle. If the particle can overcome the secondary repulsive barrier, or if that repulsive barrier is not present, it can be trapped temporarily in a secondary attractive minimum. If the shear stresses are sufficiently high, the particle will overcome the potential barrier and will flow. At rest, Brownian motion causes random movement of the small particles, causing an increased number of particles being captured in an energy well, if the repulsive forces are sufficiently low to allow this process. In this case, the particles can form groups (flocs) of connected particles and the internal structure of the suspension increases [15] [21] [22]. During shear, these connections are broken, and the internal structure decreases. The rheological properties of the material: yield stress and plastic viscosity are a function of the internal structure: the more structure, the higher these properties [25].

The second mechanism which causes the rheological properties to vary with time is of chemical nature: the hydration process between cement and water. Although hydration is minimal during the induction period, it is non-negligible. Hydration products are precipitated on the surface of the particles, and when these products overlap, the particles are connected, increasing the rheological properties [17]. Furthermore, when dispersing admixtures are used, the hydration products overgrow the molecules of the admixture, rendering them less

efficient over time [27] [28]. In the end, the transition of a cement-based material from a fluid to a solid is the result of many hydration products overlapping, creating one strong entity of particles.

The timescale of flocculation and hydration is of the order of seconds and minutes, respectively [17]. In fact, the timescale for flocculation is so small that it will affect rheological measurements of steady-state properties. On the other hand, these small timescales are also beneficial for the slipforming process, as rheological properties must increase quickly with time.

2.3 Procedures for Measuring Rheological Properties

In this section, the most common procedures which are employed to measure the steady-state and time-dependent rheological properties are discussed.

2.3.1 Measuring steady-state properties

A flow curve is typically measured when the rheological properties need to be determined. The procedure determines the stress or shear rate response due to increase or decrease in shear rate or stress, respectively [13]. The imposed signal can be either continuously varying, or can be a stepwise function. The change in the imposed parameter with time can be logarithmic or linear. For cement-based materials, a linear procedure is most commonly used. For measurements on concrete or mortar, the majority of commercially available rheometers impose a stepwise function of the rotational velocity (which can be related to the shear rate) [25]. For cement pastes, as the used rheometers are the same as in other rheological fields, there are more choices for the procedure. Linear ramps and stepwise functions are employed.

Rheometers typically do not measure shear stress or shear rate, but they measure derivate units, such as torque and velocity. The measured relationship between torque and velocity, for example, is dependent on the rheometer configuration. Relationships between shear stress and shear rate are not. As a result, shear stress and shear rate are called fundamental units. Many equations are available in literature to transform non-fundamental units to fundamental units [13]. However, for cement-based materials, as most measurements are in a linear scale and the material shows a yield stress, the equations from standard rheology textbooks are hard to apply. Alternatives have been developed, for example the integration approach. These equations are better known as the Reiner-Riwlin equations [25] [29].

However, there are a number of issues which need to be controlled during rheological measurements. The time-dependent behavior can influence the results: the mixture must be in equilibrium, which means that the rheological properties remain constant over the (short) observed time period, before a flow curve measurement can start [30] [31] [32]. Roussel has defined the reference state as the equilibrium state corresponding to the highest shear rate employed [15]. That is why a majority of flow curve measurements on cement-based materials consist of a pre-shear period at the highest shear rate, followed by a decrease in shear rate. Secondly, due to the yield stress, plug flow may occur when using a concentric cylinders rheometer [25] [31] [32]. This means that a part of the material is not sheared and an iterative procedure must be employed to calculate the rheological properties. The third measurement artifact is particle migration, as particles can move from zones with high shear rates to zones with low shear rates [33]. The chance for particle migration increases with increasing particle size and decreasing viscosity of the material. Particle migration is hard to detect, but it can make the entire measurement invalid.

2.3.2 Measuring time-dependent properties

The time-dependent rheological properties can be divided in reversible and non-reversible evolutions. However, the distinction between reversible and non-reversible depends on the applied maximum shear stress or shear rate. Furthermore, flocculation and hydration can both cause reversible and non-reversible connections between the particles.

To determine the non-reversible evolution of rheological properties with time, which is also defined as the workability loss, flow curves can be measured at fixed time intervals, employing the same procedure every time.

To measure the reversible evolutions, better known as thixotropy, different procedures can be employed.

2.3.2.1 Stepwise change in shear stress or shear rate

In this method, the sample is subjected to stepwise changes in shear rate or shear stress until the steady state or equilibrium state is reached [24]. Khayat et al. [34] [35] [36] [37] [38] developed this method, also known as the structural breakdown area method, where variations of shear stresses over time were obtained at a given set of rotational speeds. The thixotropy is quantified by the difference between the maximum initial stress and shear stress at equilibrium for a given time duration. This difference of initial stress and equilibrium stress is an indication of the magnitude of structural modifications inside the material, as suggested by Lapasin et al. [39]. In this method, the initial peak yield stress (τ_i) corresponds to the initial structural condition and, with maintained shear rate, the shear stress decreases with time reaching equilibrium (τ_e). The structural breakdown area (A_b) is the area covered between initial stress values and equilibrium stress values for different rotational speeds, as shown in Figure 1. Ahari et al. [40] also used the structural breakdown area method to evaluate thixotropic properties of SCC mixtures containing various supplementary cementitious materials. In this method, two varying parameters, namely time and shear rate provide good understanding in analyzing thixotropic models [24] [41]. However, the value of the breakdown area has no physical meaning and the result is dependent on the measurement procedure employed [41].

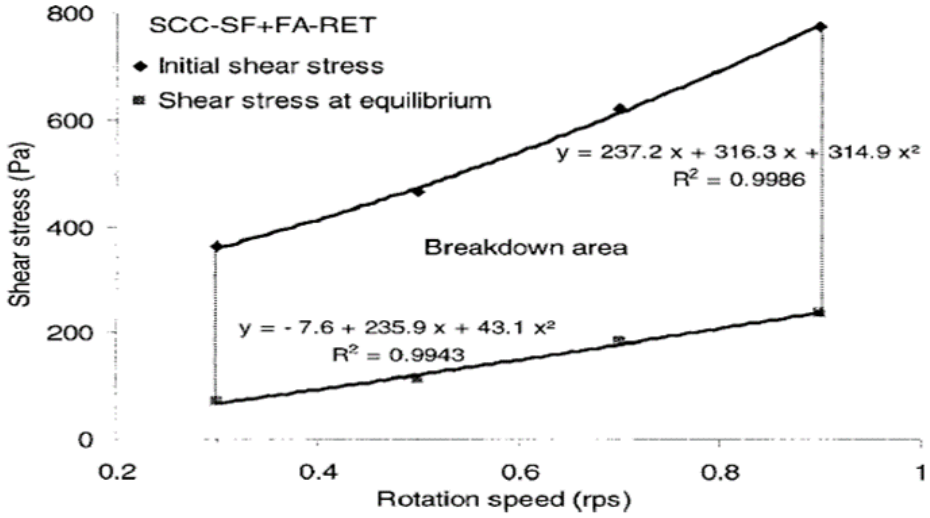

Figure 1. Determination of breakdown area obtained by initial torque responses at each rotational velocity and the equilibrium torque values [35].

2.3.2.2 Hysteresis loop curve

One of the more popular ways to quantify thixotropy of cement paste is to conduct a hysteresis loop test. In this method, a hysteresis loop is formed by increasing and decreasing the shear rates as shown in Figure 2. The area enclosed by both the up and the down curve, as shown in Figure 3, relates to the energy required to break the flocculated structure and to measure thixotropy [15] [24] [42] [43].

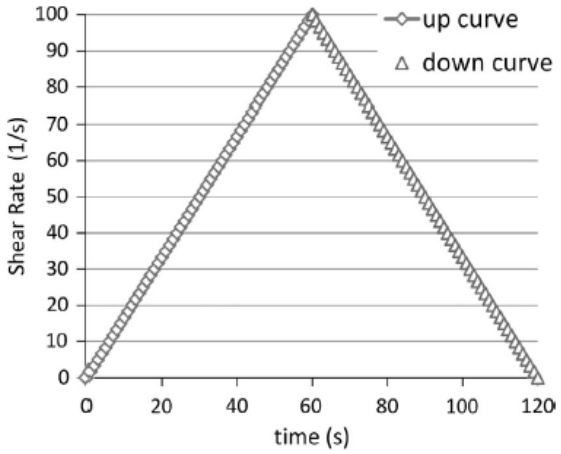

Figure 2. Shear rate history for hysteresis loop curve test [6].

However, the area and shape of the loop can vary significantly according to the material, shear history, and procedure [24] [41] [42] [43]. Roussel [15] stated that this method does not provide an intrinsic value of any physical rheological parameter. Barnes [42] and Mewis and Wagner [24] also mentioned that the test procedure and response are both based on the chosen time and shear rate, making the outcome dependent on the procedure. More uncertainties and inaccuracies of hysteresis loop method have been explained in detail in [15] [24] [41] [42] [44].

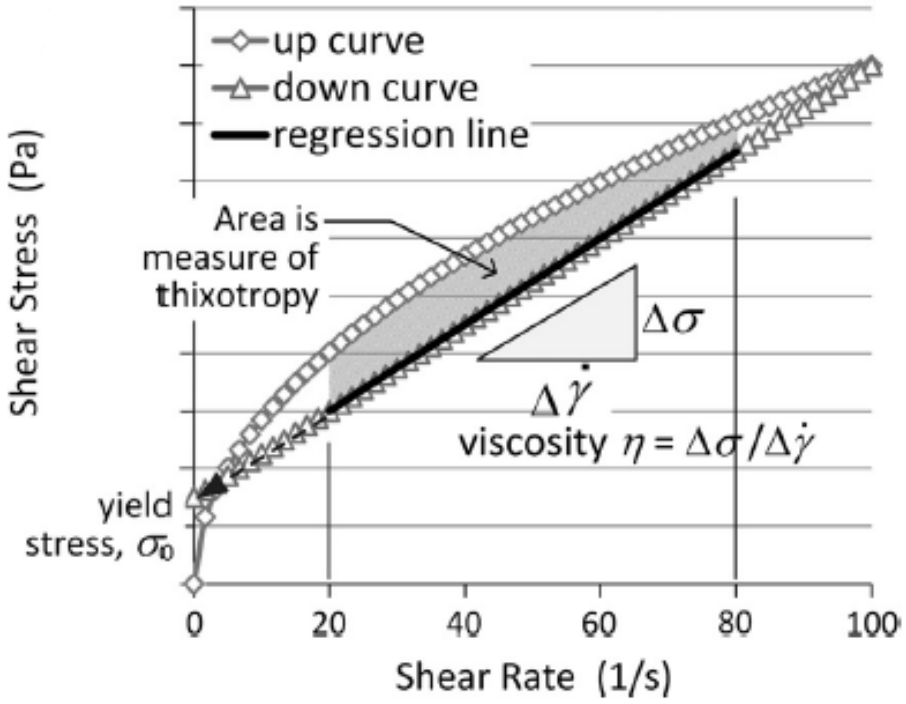

Figure 3. Cement paste hysteresis loop [6].

2.3.2.3 Static yield stress test

Thixotropy can be easily assessed by the increase in static yield stress with resting time due to build-up of structure in the material [15] [41] [43] [45]. To understand the influence of thixotropy on formwork pressure, multi-layer casting, and static stability, Roussel [15] [46] indicated that flocculation at rest is more important than de-flocculation under flow. Billberg [43] introduced a unique method to determine thixotropy of SCC

by measuring the dynamic rheology (flow curve) before and after the resting period and measuring static yield stress in every 10 min interval. This method separates the irreversible loss of workability from reversible thixotropic behavior. This phenomenon can also be explained by means of Figure 4 [43]. The static yield stress increases linearly under a resting condition, whereas the dynamic yield stress showed negligible change. Similar behavior was also observed by Ovarlez and Roussel [45]. This linear increment in static yield stress of cement paste and flowable concrete is transformed into a simple equation by Roussel [15], in which, at rest, shear rate is zero and the growth of the apparent yield stress is according to the following equation (Eq. 3).

$$\tau = \tau_0 + A_{thix}t \qquad \textit{(Eq. 3)}$$

where, τ = shear stress (Pa)
τ_0 = static yield stress (Pa)
A_{thix} = characteristic time for structuration of cement paste or concrete (Pa/s)
t = time (s)

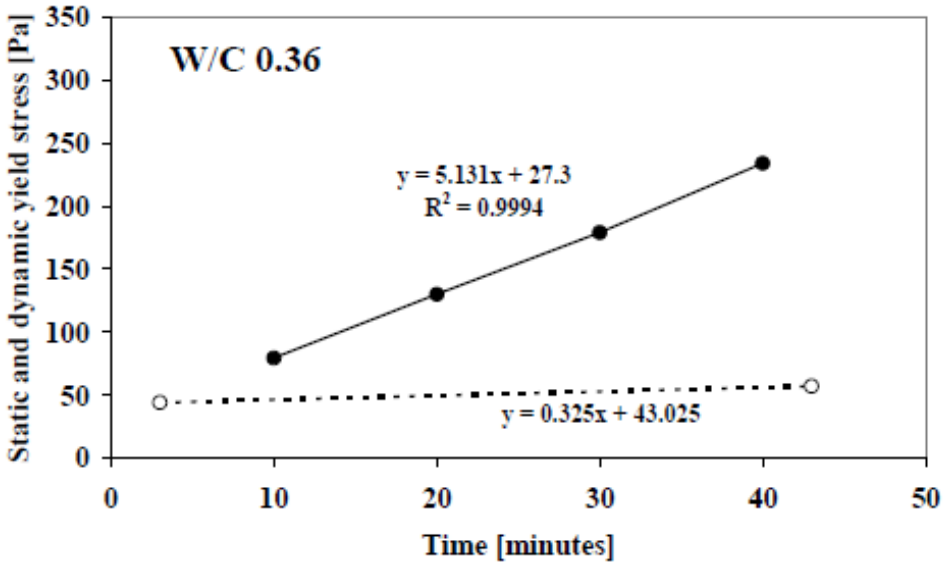

Figure 4. Linear increment in static yield stress over a time under a rest. The solid line represents the static yield stress and the dashed line is the dynamic yield stress which only increases due to the workability loss [43].

2.4 Other Test Methods Used for Vibration-Free Concrete for Slipforming

2.4.1 Slump flow and flow table tests

The slump flow test method for conventional SCC was used to evaluate the flowability of VFC for slipforming mixtures according to ASTM C1611 [5] [6]. The flowability of paste or concrete mixtures was evaluated by the flow ratio using the flow table test, according to EN-206 and ASTM 1437, by Voigt et al. [47] and Pekmezci et al. [11], respectively. The flow ratio is defined as the ratio of the diameter of the concrete cone at the base before and after the material was subjected to the desired number of drops. Pekmezci et al. [11] studied flowability by applying 25 drops of the drop table, while Voigt et al. [47] conducted the flowability test on a two plate drop table, in which the plate was dropped 15 times from a 40 mm height. Wang et al. [5] evaluated the flowability of paste or mortar according to the flow table test described in ASTM C230 and final flow was obtained after 18 drops.

2.4.2 Shape stability or green strength tests

Breitenbucher et al. [48] determined the shape stability of paste and mortar by means of the mini slump cone test. A slump cone with an upper diameter of 70 mm, a height of 60 mm, and a base diameter of 100 mm was filled with fresh paste. The shape stability was evaluated 5 minutes after the initial mixing and after re-mixing of the mixture at 10 minutes. The height (h), the top diameter (d) and bottom diameter (D) of the paste or mortar after removal of the cone were measured.

The shape stability of concrete was also determined using a standard cubical formwork (150 x 150 x 150 mm^3). The shape stability coefficient of fresh paste or mortar, K_p, and concrete, K_c, was measured from equations 4 and 5, displayed in Figure 5 left and right, respectively. Similarly, Hoornahad et al. [49] evaluated the shape stability by determining the shape preservation factor (SPF). SPF is the ratio of the vertical cross-sectional area of the sample before and after demolding i.e. A_f/A_o.

$$K_p = \frac{11}{(D+d-h)} \quad \textit{(Eq. 4)}$$

$$K_c = \frac{15}{(w+l-h)} \quad \textit{(Eq. 5)}$$

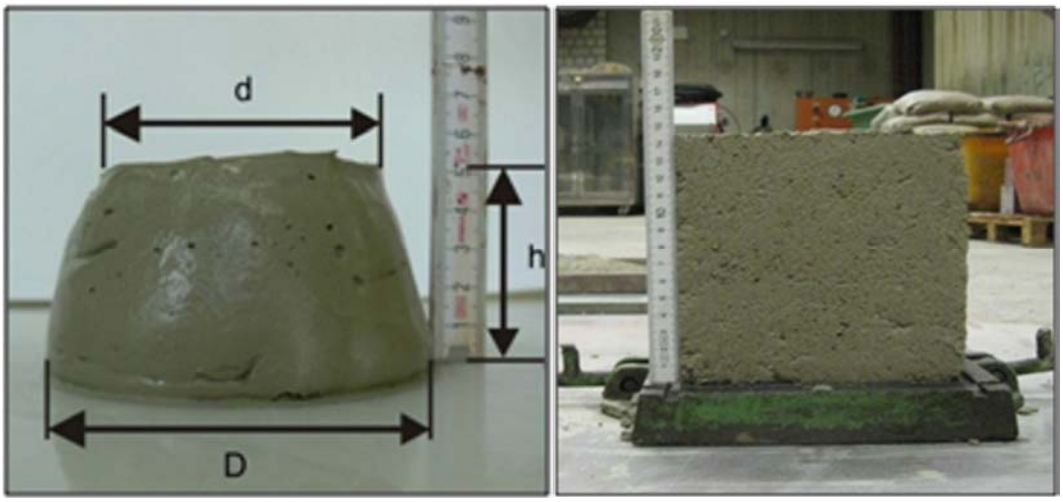

Figure 5. Left: Shape stability of paste/mortar test specimen with equation 4. Right: Shape stability of fresh concrete test specimen with equation 5 [48].

Breitenbucher et al. [48] evaluated the green strength of a concrete cube which consists of a lever beam centered on the demolded concrete as shown in Figure 6. A bucket at the other end of the lever beam was filled continuously with sand until a deformation of 10 mm in the concrete was reached. The mass of the sand in the form of load was measured to determine green strength of concrete. However, Voigt et al. [47] and Pekmezci et al. [11] evaluated the shape stability using a modified flow table method. A 100 mm x 200 mm loosely filled concrete cylinder was consolidated with 15 [47] or 25 [11] drops on the flow table. Then, the cylinder was demolded and loaded slowly but continuously with a small amount of sand until the sample collapsed, as shown in Figure 7. Wang et al. [5] evaluated the green strength using a simple sand method, as shown in Figure 8. In this method, the VFC mixture was poured into the small cylinder mold (100 mm x 127 mm) at a height of 300 mm. After the casting, the formwork was removed immediately and a cylinder showing small or no deformation was considered further for the green strength evaluation. A plastic cylinder (150 mm x 150 mm) was placed on top of the cylinder and gradually filled with sand until the specimen collapsed. The total quantity of sand used (load) during the test divided by the loading area of the sample is defined as the green strength of the concrete.

Figure 6. Test setup for the green strength from Breitenbucher et al. [48].

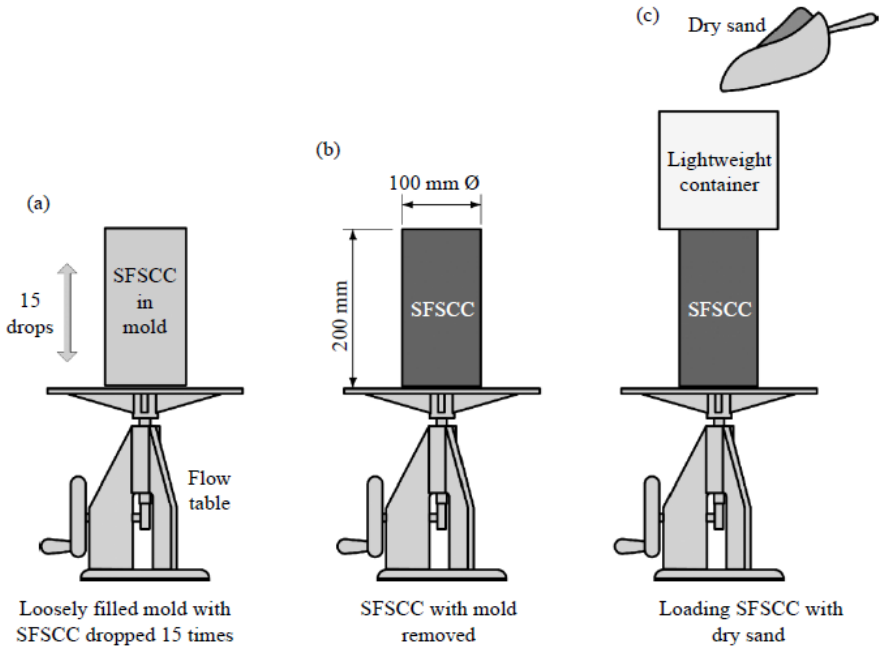

Figure 7. Green strength test setups according to Voigt et al. [47] and Pekmezci et al. [11]. SFSCC stands for slipform SCC, which is similar to the VFC term used.

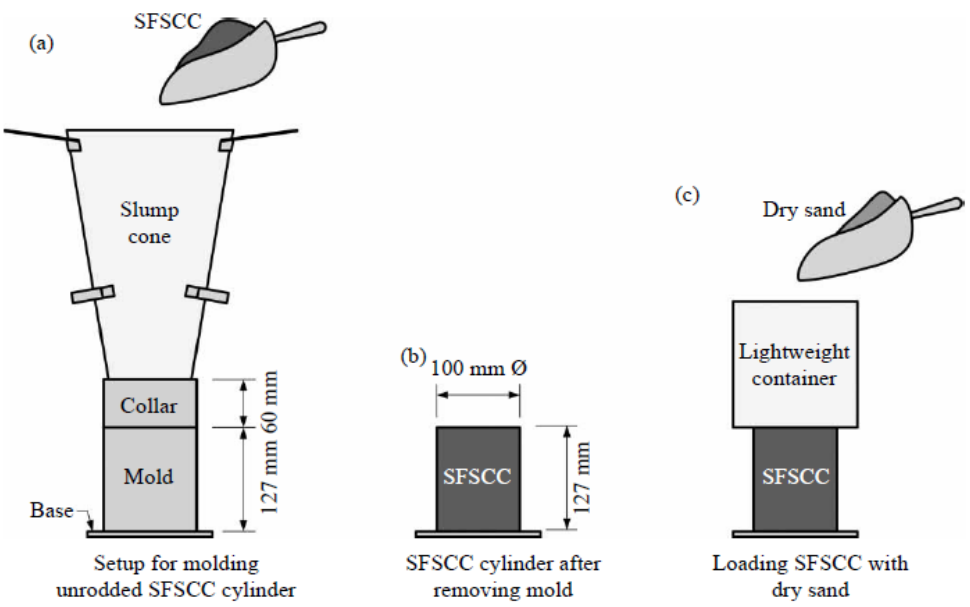

Figure 8. Green strength test setups according to Wang et al. [5].

2.4.3 Mini-paver test

To simulate the field slip form paving method in the lab, a mini-paver test [5], [11], [47], [50] system was developed. It is comprised of three parts: (1) L-shaped box with a platform on top; (2) a towing system; and (3) a working table, as shown in Figure 9. Initially, concrete was placed on the platform as shown in Figure 9 (left) and pushed up to a certain height through the vertical leg of the L-box to consolidate the mixture. Then, the mini-paver was pulled forward with crank system at a designed speed of 1.5-2.5 cm/s. Lastly, as the mini-paver moved forward, the concrete slab was extruded out of the horizontal leg of the L-box as shown in Figure 9 (right). The surface quality and the edge slump of the concrete slab resulting from the mini paver indicated the consolidation, shape holding ability and ultimately the feasibility of the SFSCC mixture for slip form pavement construction [8].

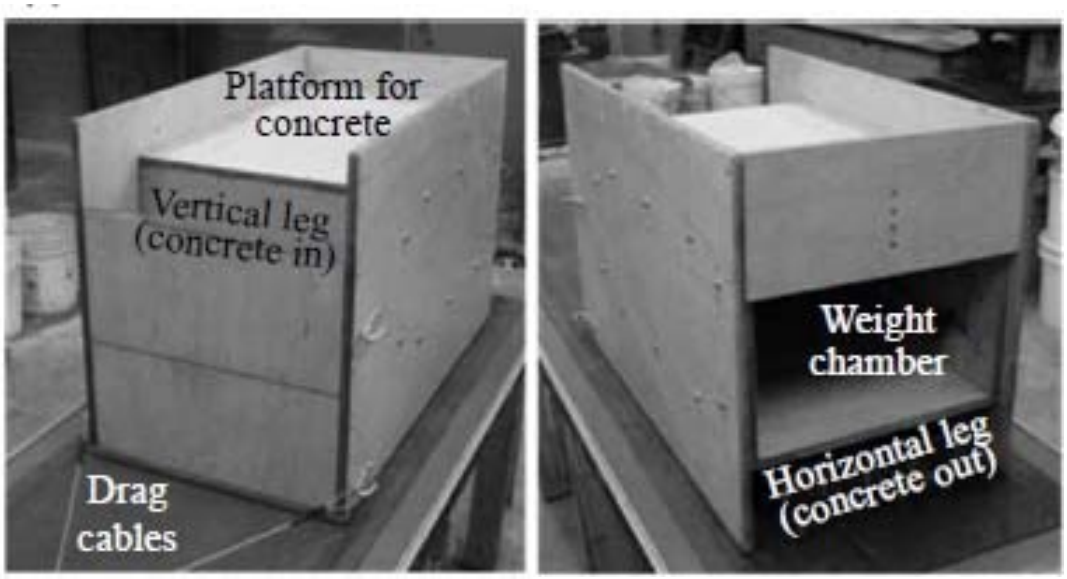

Figure 9. Mini-paver system [5] [6] [11] [47].

2.4.4 Compaction factor test

The self-consolidating ability of the SFSCC mixture was evaluated by the modified compaction factor test method [6] as shown in Figure 10. In this method, a cylinder (100 mm x 200 mm) was filled with freshly mixed concrete through an inverse slump cone under its own weight. The unit weight of the concrete specimen was then determined and compared with unit weight of the concrete specimen obtained with three layers and rodded 25 times for each layer. The ratio of the unit weight of loosely filled concrete to the unit weight of compacted concrete is defined as the compaction factor. A compaction factor close to, or equal to 1 represents a good self-consolidating concrete [6].

Figure 10. Compaction factor test setup [6].

2.5 Mix Design Factors Affecting Critical Properties of Vibration-Free Concrete for Slipforming

This section gives an overview of the mix design factors which affect fresh / rheological properties critical for slipforming of vibration-free concrete. The overview focuses on main factors influencing rheology and in particular thixotropy, while green strength and shape stability are also discussed.

2.5.1 Effect of paste constituents on rheology, and in particular, thixotropy of cement-based materials

Seen the necessity for rapid stiffening of the concrete mixtures, thixotropy needs to be maximized. Thixotropy of concrete and thixotropy of cement paste are related, as the mechanisms of thixotropy are in the cement paste, although a remark will be made on that aspect in the analysis of the experimental work on concrete mixtures, discussed further in this report.

2.5.1.1 Water-to-binder ratio

Topcu and Uygunoglu [51] investigated the effect of different binders with varying w/b ratio and superplasticizer (SP) content on yield stress of self-consolidating mortar. They reported that yield stress decreases and flowability increases with an increase in w/b ratio and SP content. Billberg [43] has also reported that with an increase in w/b ratio from 0.34 to 0.42 the structural build-up, i.e. consequences of thixotropy, decreases by almost 80%. He mentioned that w/b ratio is related to the particle concentration and decreasing w/b lowers the interparticle distance, resulting in quicker structural build-up. Furthermore, Rahman et al. [52] stated that thixotropy increases with an increase in binder content when sand and coarse aggregate content is low. Also, w/b ratio influences the average distance between the particle and their interaction level, leading to an increase in thixotropy with a decrease in w/b ratio. Roby [53] indicated that an increase in w/b ratio increases the lubrication of cement paste and decreases the cohesiveness of the mixture. Assad and Khayat [54] [55] further stated that mixtures with higher w/b ratio and lower coarse aggregate proportion show a reduction in internal friction and increase the mobility of the mixture, yielding higher initial lateral pressure and slower thixotropy development. Thus, it is obvious that an increasing w/b ratio results in a decrease of thixotropy of concrete mixture.

2.5.1.2 Cement properties

According to Nunes et al. [56], the workability is influenced by different cement deliveries and cement-superplasticizer interaction should be studied for different cement deliveries in SCC mixtures. The authors further mentioned that changes in rheological properties are mainly caused by differences in cement fineness and the sulphate amount of cement. Juvas et al. [57] reported the workability of mortars with superplasticizer is substantially more sensitive than for mortars without superplasticizer. Quanji [58] stated that cement pastes with high alkali content yield faster structural rebuilding rate potentially due to the increase in bond strength of particles by the pore solution chemistry. Also, it enhances prismatic crystal formation ability which enhances interlocking of microstructure and increases the structural rebuilding rate.

2.5.1.3 Effect of supplementary cementitious materials and mineral fillers

A small addition of nanoclay, which is a thixotropy enhancing material, has the ability to improve thixotropy [59] and shape stability [11] [60] of VFC for slipforming. Wang et al. [6] studied the thixotropy of cement paste with an increase in attapulgite clay (0.5%, 1%, 2%, 3%), a nanoclay, using a hysteresis loop method. Results showed that increasing the amount of attapulgite clay increases thixotropic development with time. The addition of attapulgite clay also increased thixotropy of cement paste combined with fly ash or the presence of HRWR (high-range water reducing agent) or AEA (air-entraining agent). Ferron et al. [61] mentioned that nano-sized particles create a more stable microstructure in concrete and work as a filler material by filling the gaps between the cement particles. Quanji et al. [62] showed that an increase in dosage of attapulgite clay not only increased the yield stress and viscosity but also enhanced the thixotropy with time. This study also confirms the beneficial effect of nanoclay on thixotropy and the effective relationship between flow percent reduction and structural rebuilding of cement paste. It was concluded that the optimum dosage of nanoclay for the effective thixotropic behavior would be a 1.3% addition by mass of cement [62]. Many researchers attributed the influence of nanoclay on improvement of thixotropy due to its surface charge [62], ability to absorb water [62], irregular microstructure [59], smaller size [61] [62] and specific surface area [61]. However, Kawashima et al. [63] reported that nanoclay has immediate effect on thixotropy due to flocculation mechanism, but this effect diminishes over a time.

Hassan et al. [64] compared the influence of metakaolin (MK) and silica fume (SF) on the rheological properties of SCC. Their results indicated that the replacement of metakaolin (up to 25%) increased the plastic viscosity and yield stress significantly by 2.4 times and 3.2 times of the reference mixture respectively (at a constant HRWR dosage 3460 ml/m^3). They also reported that 8% SF had less effect on viscosity but, 8% SF had more influence on yield stress compared to 8% MK. Güneyisi and Gesoğlu [65] investigated the influence of binary and ternary mixtures using fly ash (FA) and MK on the rheology of self-compacting mortar. The addition of MK enhanced the viscosity while FA decreased the viscosity. They also mentioned that a combination of both FA and MK can be modified to achieve required yield stress and viscosity. The cement pastes studied by Wang et al. [5] showed that fly ash (class C and F) decreased the yield stress and viscosity compared to a mixture with 100% cement, whereas 30% slag replacement increased both the viscosity and yield stress.

Rahman et al. [52] studied the thixotropic behavior of SCC containing mineral additives and SCMs such as limestone powder (LSP), silica fume (SF), and fly ash (FA) by means of the static yield stress method proposed by Roussel [15]. They found a significant increase in thixotropy (A_{thix}) with an increase in the amount of fly ash from 5% to 10% whereas silica fume showed the opposite trend. LSP had less impact on thixotropy. All binary mixtures in the study [52] showed higher thixotropy index than the reference SCC mix because of higher fineness and structuration rate. Rahman et al. [52] further showed that A_{thix} can be used to determine the suitability of mix designs for particular SCC applications. SF mixtures could be applied for horizontal construction and FA mixtures could be selected for the construction of walls. Assaad and Khayat [35] investigated the thixotropic and rheological properties of SCC using silica fume (SF), fly ash (FA) and blast furnace slag (BFS). They reported that binary (PC + SF), ternary (PC + SF + FA) and quaternary systems

(PC+SF+BFS+FA) showed lower plastic viscosity and higher thixotropy values compared to plain SCC mix during the initial 30 min. Later, after re-mixing a decrease in thixotropy was noticed in the quaternary mixture until 150 min. Ahari et al. [40] reported that SCMs such as FA and MK led to an increase in plastic viscosity irrespective of the w/b ratio, whereas SF and BFS led to decrease in plastic viscosity.

2.5.1.4 Effect of dispersing admixtures (HRWRA)

There are some research studies available regarding the influence of superplasticizer on the development of thixotropy. Ore et al. [66] have shown the limited influence of incorporating a water-reducing agent on thixotropy. However, Ferron et al. [61] reported that the use of superplasticizer for adoption of a lower w/c in pastes is the most effective method to enhance the rate of structural build-up. Billberg [43] found that electrostatic hindrance mechanism of melamine SP showed more structural buildup than steric hindrance mechanism of PCE (poly carboxylate ether)-SP. Adding a HRWRA to enhance workability was reported to increase formwork pressure and thus decrease thixotropy [53] [55], while for a given slump, reducing w/c ratio by using HRWRA developed similar formwork pressure as that of concrete made without HRWRA [53] [55]. Wang et al. [6] indicated that the addition of HRWR and AEA in cement paste made with FA and attapulgite clay decreases thixotropy and viscosity. Roussel et al. [46] have indicated that for a polycarboxylate-based superplasticizer, by increasing the amount of superplasticizer in the mixture, the structuration rate (A_{thix}) decreased.

2.5.1.5 Effect of viscosity-modifying admixtures (VMA)

Viscosity-modifying admixtures are mostly used along with a high-range water reducing agent to control cohesiveness and increase the stability [67]. The thixotropic behavior of cement pastes is related to the interactions between solid particles and the water medium containing chemical admixtures such as HRWRA and VMA [52] [56] [57]. Thixotropic properties were measured by considering the influence of HRWRA and VMA combinations on concrete-equivalent-mortar with equivalent fluidity and by using a parallel plate rheometer [68]. Results [68] showed that powder or liquid polysaccharide-based VMAs develop greater initial static shear stress needed to breakdown the structure after resting time compare to cellulose-based VMA. On the other hand, a higher degree of flocculation has been reported in mixtures containing combinations of VMA with naphthalene-based HRWRA compared to combinations of VMA with polycarboxylate-based HRWRA [68]. In addition, Assaad and Khayat [54] indicated that in SCC made with w/b of 0.36 and ternary cement (6% silica fume, 22% Class F fly ash, and 72% Type 10 (GU) Portland cement), combining cellulose based VMA with PCE-HRWRA led to higher thixotropy compared to mixtures containing polysaccharide-based VMA and poly-naphthalene sulfonate (PNS) HRWRA.

Assaad and Khayat [37] concluded that a combination of cellulose-based VMA along with polycarboxylate-based HRWRA increased the degree of thixotropy of SCC compared to mixtures containing powder or liquid polysaccharide-based VMA and naphthalene-based HRWRA. However, the SCC mixtures containing cellulose-based VMA with polycarboxylate-based HRWRA showed a lower rate of increase in thixotropy with time due to its fluidity retention property [37]. Van der Vurst et al. [69] investigated the influence of four different VMAs (attapulgite clay, diutan gum, corn starch, and propylene carbonate) on the robustness of SCC mortars. Their results showed that maximum robust yield stress was found in mixtures without VMA and mixtures with attapulgite clay. Also, diutan gum had highest plastic viscosity while attapulgite clay and corn starch displayed no effect on the plastic viscosity. Helnan-Moussa et al. [70] presented a semi-empirical procedure to evaluate the structural breakdown of fresh cement pastes with different amounts of viscosity-modifying admixture (VMA). A stepwise decreasing shear rate sequence was applied after a constant high pre-shear. Results indicated that, beyond a maximum value of VMA, cement pastes form tri-dimensional networks that are significantly flocculated and thus show more difficulty to deflocculate by shearing [70].

2.5.2 Effect of paste constituents on shape stability and green strength

The evaluation of fluidity and stability of SCC are important concerns for slip forming. Few researchers have investigated the factors affecting the balance between flowability and shape stability (green strength) of mixtures requiring low compaction energy. Shape stability, i.e. green strength, can be defined as the ability of the mixture to support its own weight in its given shape. It is the crucial parameter in slip form paving where no formwork is used. Breitenbucher et al. [48] investigated the effect of SCMs, clays and thixotropic agents on the slump flow and shape stability of paste, mortar and concrete mixtures for slip form pavement applications. The authors investigated two different approaches to develop concrete mixtures with good flowability and high shape stability. One approach was to add thixotropic agents in the original mixture to develop a thixotropic concrete. This concrete shows consistent flowability during transport and placement, while viscosity increases with time after casting. In this approach, mineral admixtures (consisting of kaolinite, illite, and quartz powder), metakaolin, bentonite, modified starch, tetrasaccharides and other modified polymers were employed as thixotropy-enhancing agents. Their investigation showed that paste with metakaolin and a polycarboxylate ether (PCE) superplasticizer reached the targeted values (shape stability coefficient (K_p) > 0.9 and mini slump flow > 200 mm). After re-mixing, to check the behavior of the mixture during delivery and casting, none of the pastes mixed with the polymeric thixotropic agent (tetrasaccharides and other modified polymers) and mineral additions (e.g. bentonite, metakaolin, modified starch) achieved the targeted values. Also, re-mixing led to a 97% reduction in green strength of concrete with thixotropic agents (modified polymer, modified starch and metakaolin).

In the other approach, Breitenbucher et al. [48] used viscosity-increasing agents to achieve sufficient shape stability and stiffening behavior. In this approach, an SCC mixture with slump flow of 700 ± 20 mm was obtained using PCE superplasticizer and when the viscosity-increasing additive was added 15 min after the initial mixing. They reported that the addition of the viscosity-increasing additive, superabsorbent polymer (SAP), with PCE superplasticizer led to a significant decrease in slump flow and a shape stability coefficient (K_c) of 0.76 to 0.79 was determined. A higher shape stability coefficient was achieved when naphthalene sulfonate (NaS) was combined with PCE superplasticizer. In a concrete mixture with 3% PCE and 1% NaS of cement weight, slump flow was reduced from 690 to 490 mm and a shape stability coefficient of 0.85 was achieved [64]. In a concrete mixture containing 3% PCE and 1.5 % NaS, slump flow was reduced from 690 to 440 mm and shape stability coefficient of 0.95 was achieved [48]. Therefore, the targeted shape stability and high flowability could not be achieved simultaneously using this approach [48].

Pekmezci et al. [11] determined the flowability and shape stability under the effect of external compaction energy, i.e., using the drop table test as explained in section 2.4.1. They discovered that more flowability was achieved in concrete mixtures with naphthalene-based (PNS) plasticizers compared to polycarboxylate-based (PCE) plasticizers, while still showing sufficient green strength. Their results also showed that the addition of an air-entraining agent (AEA) to attain enhanced air-void structure does not affect the flowability and green strength of the mixture. Moreover, adding clay minerals up to 1% of attapulgite clay and 1.5% of metakaolin of cement weight proved to be beneficial in modifying flowability with effective green strength development. However, concrete mixtures containing VMA or kaolinite provided higher green strength with a small loss in flowability. The work of Pekmezci et al. [11] and Voigt et al. [47] also indicated that the incorporation of fly ash and a naphthalene-based superplasticizer (PNS) led to an increase in flowability but showed negative impact on the green strength. Pekmezci et al. [11] attributed this higher flowability behavior of concrete due to the spherical shape, finer size and lower specific gravity of fly ash. Also, for a given water/binder (w/b) ratio, fly ash decreased the water demand causing an increase in flowability [71].

Voigt et al. [47] investigated the effect of clay minerals and fibers in fly ash-modified SCC (replaced 30% of cement weight) (SCCF) mixtures to achieve the required balance between flowability and green strength. They reported that attapulgite clay displayed a maximum green strength (2.4 kPa) with minimal negative impact on flowability. SCCF with other clay minerals, MgO and fibers showed similar green strength (1.3-

1.8 kPa). SCCF with polypropylene fibers showed maximum flow ratio among all SCCF mixtures. The relationship between the green strength and flowability is shown in Figure 11 [11]. From these results, a general trend can be observed: as the flow ratio increased, the green strength value decreased. However, some concrete mixtures followed a different trend, i.e. for a given flow ratio, a plain mixture with naphthalene-based plasticizer (Plain (naphth) in the figure), the mixtures with fly ash (FA) and clay minerals and mixtures containing VMA and AEA, displayed higher green strength values. These mixtures may be considered as potential candidates for concrete requiring reduced or no consolidation energy.

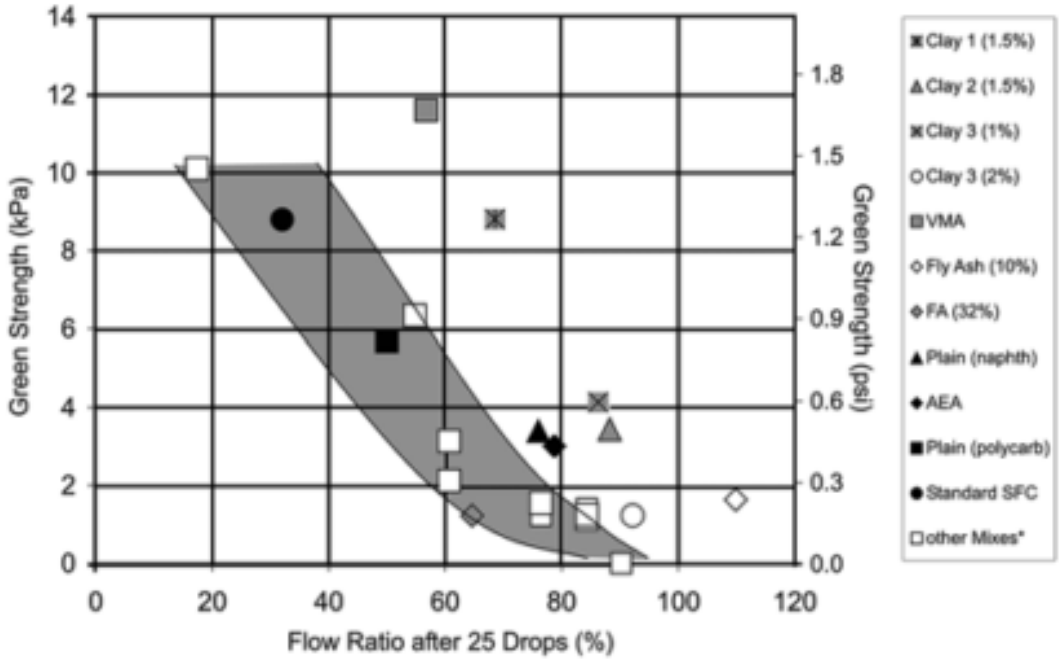

Figure 11. Relationship between green strength and flowability (flow diameter after 25 drops on drop table) [11].

From the mini paver tests, it has been observed that all concrete mixtures with clay minerals and fibers improved the edge stability, while good surface quality without any internal or external vibration was observed [11] [47].

In an accelerated slab replacement study, Armaghani et al. [72] reported that SCC mixtures with four admixtures i.e., HRWR, slump retaining admixture, regular water reducing admixture and set retarder (Type D according to ASTM C494), and accelerator, displayed high workability retention without segregation. They stated that workability was retained for one hour after adding the accelerator. Their results also showed an effective early age strength of 54 MPa (1 day) for a given SCC mixture, which is more than what is required for accelerated slab replacement application.

Wang et al. [73] reported that SCC mixtures for slipforming with higher replacement of cementitious materials (40%FA+15%MK), with and without nano-limestone, resulted in good flowability and shape stability, thus satisfying the design criteria. Garg and Wang [74] studied the performance of mortars containing a combination of three clays and fly ash. They concluded that all three clays decreased the flowability of the mortars and an optimum amount of attapulgite clay can be helpful in improving shape stability of concrete for slip form pavement application. Attapulgite clay led to a significant reduction in flowability due to its high water adsorption capacity [69] [75] and thixotropic behavior [58]. Tregger et al.

[60] also concluded that an increase in stiffness resulted in concrete mixtures containing attapulgite clay having the highest green strength compared to other clay additives.

Garg and Wang [74] reported that a higher content of metakaolin led to a significant decrease in flowability [76], caused by the imbalance between the extra fine particles and a lack of water. Ge et al. [77] found that the incorporation of nano-limestone resulted in a decrease in slump flow while an increase in particle size of nano-limestone led to increase in slump flow. The fly ash-cement mortar study conducted by Kawashima et al. [78], concluded that flowability increased with the addition of fly ash, while it decreased with addition of CNS (colloidal nanosilicate). Modification in particle shape, size and paste volume of SCMs and clay minerals causes variations in the dosage of superplasticizer required to reach a target slump flow value. Han et al. [79] found that in high-strength SCC mixtures, the addition of SRA (shrinkage reducing admixtures) and SAP (super-absorbent polymers) lowered the flowability requiring an adjustment of the HRWR dosage.

2.5.3 Effect of aggregates

For concrete mixtures with an aggregate content under the threshold for friction [14], aggregates typically amplify the paste behavior, mostly in accordance with a Krieger-Dougherty style of equation (see Eq. 6) [80] [24] [81]. For mixtures with aggregate contents above the threshold for friction, no large concrete flow can be obtained [14]. As such, these mixtures are not included in the investigation. The amplification of cement properties caused by the aggregates is non-linearly proportional to the ratio of the volume fraction of aggregates in mortar or concrete and the maximum volume fraction, or maximum packing density, of these aggregates. These principles are strongly employed in studies on ecological concrete, where constant flowability is desired with a decreasing binder content. Typically, the aggregate grain size distribution is optimized to maximize the maximum packing density.

$$\eta_s = \eta_m \left(1 - \frac{\varphi}{\varphi_{max}}\right)^{-[\eta]\varphi_{max}} \qquad \textit{(Eq. 6)}$$

where: η_s = viscosity of the suspension (Pa s) (mortar or concrete)
η_m = viscosity of the medium (Pa s) (paste)
φ = volume fraction of solid particles (-) (aggregates)
φ_{max} = maximum packing density of the solid particles (-)
$[\eta]$ = intrinsic viscosity of the particles (-) (relates to the shape, angularity of the aggregates)

Maximum packing density of granular materials can be measured by means of the Gyratory compactor testing equipment, also known as the intensive compaction tester (ICT). It is a popular equipment to investigate the compactibility and stability of zero-slump concrete or conventional pavement concrete. The ICT consists of a test cylinder, a piston, and an electronic pressure device. It calculates the density of the specimen by continuously measuring the height during the compaction of the cylinder subjected to shear movement and constant pressure (commonly known as compaction cycles) [82]. Mueller et al. [83] and Khayat and Mehdipour [84] recently proposed that the ICT is a simple and effective tool to determine the maximum packing density of solid particles of SCC mixtures, including aggregates [84] or aggregates and cementitious materials [83].

Geiker et al. [85] investigated the effect of coarse aggregate volume fraction and shape on the rheology of SCC. Their results showed that not only volume fraction but also the aspect ratio, angularity, shape, and surface texture of coarse aggregate influence the yield stress and viscosity, as they influence the maximum packing density. Koehler [86] reported that natural aggregates, well-shaped crushed coarse aggregates, and well-shaped manufactured sands showed low interparticle friction, causing low HRWRA demand, and low plastic viscosity. Jovein and Shen [87] reported that for SCC mixtures at w/c = 0.35 and slump flow ranging between 580 mm to 740 mm, increasing aggregate volume resulted in higher static and dynamic yield stress. Their results also confirmed the Krieger-Dougherty type of model [81] relating the mixture yield stress to the

yield stress of suspending fluid similar to Eq. 6, which implies increasing aggregate volume increases yield stress of the mixture.

Based on the principles of volume fraction and maximum packing density, the excess paste layer concept was developed by Kennedy [88] in 1940 to explain the driving factor influencing the workability of concrete. According to this theory, the total paste volume is divided into a paste volume to fill the voids between the aggregates, and an excess paste volume to cover the surface area of the aggregates to achieve desired workability. This excess paste thickness reduces the inter-particle friction between the aggregates and improves the workability of the mixture. Concrete with an aggregate system without excess paste layer moves when overcoming the friction between the particles, while aggregate voids filled with paste and an excess paste layer modifies the interaction between the aggregate from inter-particle friction to a lubricating effect. In this case, the mobility of aggregate particles is enhanced. Hoornahad et al. [49] and Oh et al. [89] systematically explained the excess paste layer system in two parts, i.e. the void paste and the excess paste. Figure 12(a) shows a total volume of a sample equivalent to the volume of aggregate and total paste volume in loose state. Figure 12(b) shows a system with bulk volume of the aggregates, consisting of the volume of aggregate and paste volume in compacted state, and excess paste volume. Lastly, Figure 12(c) shows a total volume of sample containing the aggregate volume, paste volume to fill the voids between the aggregate, and the excess paste volume. The excess paste volume can be calculated as follows:

$$V_{pex} = V_p - V_{pv} \quad \textit{(Eq. 7)}$$

$$V_{pv} = \left(\frac{1}{\varphi_{max}-1}\right) V_a \quad \textit{(Eq. 8)}$$

where: V_{pex} = excess paste volume
V_p = paste volume
V_{pv} = paste volume necessary to fill the voids in between the aggregates in maximum packing
φ_{max} = maximum packing density
V_a = volume of aggregates

It can also be said that for a given paste volume, a higher maximum packing density of the granular system provides a higher excess paste amount than what is required to fill the voids between the aggregates, and as such, a thicker paste layer coats the aggregates. Thus, a granular system with a high maximum packing density with a sufficient excess paste layer is beneficial for better flowability due to lower inter-particle interaction. The correlation of excess paste layer thickness to flowability of fresh concrete is also confirmed by Denis et al. [90] and Kwan and Li [91]. Kwan and Li [91] reported that the fines in the aggregate (particles finer than 75 μm) are considered a part of the paste volume. To develop concrete mixtures with good shape stability and flowability, without compromising its self-consolidating characteristics, a sufficiently large paste volume is required, which will not only fill the voids between aggregates but also provide a sufficiently thick paste layer to ensure adequate flowability [6] [49]. Hoornahad et al. [49] stated that paste consistency (ability to flow) is significantly controlled by the amount of superplasticizer and an increase in excess paste volume causes the yield stress and shape preservation factor (shape stability) to decrease.

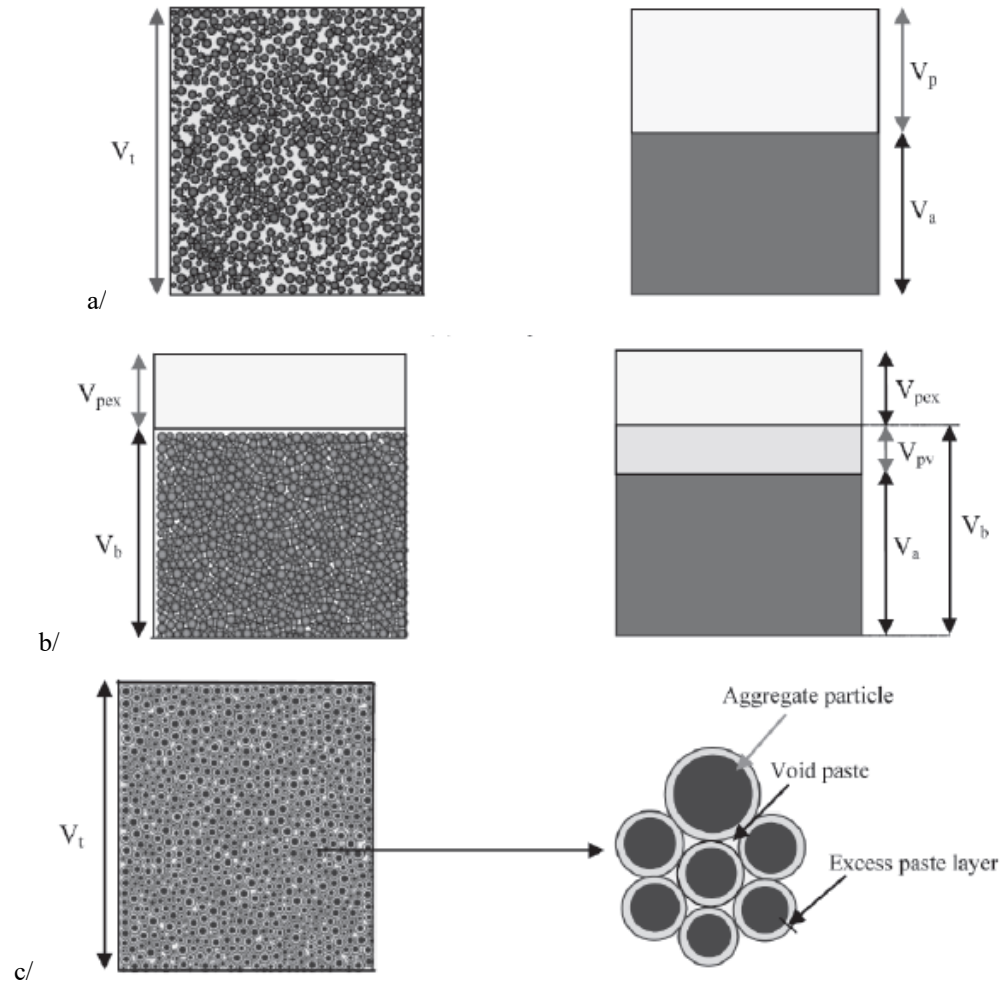

Figure 12. Two phase aggregate-paste system in the excess paste layer where, V_t, V_a, V_b, V_p, V_{pv} and V_{pex} are volume of the sample, specific volume of the aggregate, bulk volume of the aggregate in compacted state, total paste volume, void paste volume and excess paste volume, respectively [49].

3 Materials and Methods

3.1 Materials

The following sections discuss the different constituent materials used in the cement paste study and those retained for the concrete portion.

3.1.1 Cement

A commercially available type I/II ordinary Portland cement has been used throughout this research work. The cement has an estimated Bogue composition of 61% C_3S, 8% C_2S, 6% C_3A, 9% C_4AF, and 3.4% of gypsum. The density is 3170 kg/m^3.

3.1.2 Supplementary cementitious materials and mineral fillers

The following supplementary cementitious materials (SCMs) and mineral fillers were employed to investigate their suitability for VFC for slipforming on cement paste level.

- Slag cement, at 25% replacement, density 2910 kg/m^3
- Limestone filler, at 10% replacement, density 2730 kg/m^3
- Silica fume, at 5% replacement, density 2390 kg/m^3
- Metakaolin, at 25% replacement, 2680 kg/m^3
- Kaolin, at 1% replacement, 2940 kg/m^3
- Nano silica, at 1% replacement, 2670 kg/m^3
- Attapulgite clay, at 0.5% replacement, delivered at a 20% solid concentration. The density of the particles is 2290 kg/m^3.

These SCMs were first employed as binary systems, after which the best performing materials were combined in ternary mixtures.

Table 1. Chemical composition and physical properties of the employed slags in the concrete study.

BASIC COMPOUNDS (%)	***CEM***	***SLAG paste***	***SLAG - A***	***SLAG - B***	***SLAG - C***	***SILICA FUME***	***ATT. CLAY***
MgO	2.77	8.10	8.65	4.77	8.30	0.43	10.30
Al_2O_3	3.35	6.84	8.57	10.90	7.13	0.81	11.60
SiO_2	16.68	34.69	32.80	29.58	35.99	96.98	63.93
SO_3	3.25	2.19	1.88	3.10	2.30	0.32	0.35
K_2O	0.57	0.37	0.37	0.32	0.39	0.73	0.65
CaO	69.01	45.70	45.93	49.41	44.09	0.29	5.84
TiO_2	0.25	0.47	0.52	0.64	0.43		0.65
Mn_2O_3	0.17	0.74	0.33	0.28	0.70	0.01	0.08
Fe_2O_3	3.62	0.55	0.70	0.25	0.45	0.11	5.02
DENSITY (kg/l)	3.17	2.90	2.85	2.73	2.72	2.39	2.29
D_{50} (µm)	15.4	14.2	13.6	13.6	11.6	0.35	0.3[1]

[1] *According to manufacturer*

For the concrete study, the best-performing combinations of materials were retained, which were slag, silica fume and attapulgite clay. For the slag cements, three additional deliveries were ordered, from three different suppliers. The chemical composition, density and d_{50} can be found in Table 1.

3.1.3 Dispersing admixtures

Two commercially available dispersing admixtures (SP) were employed: one polycarboxylate-based (PCE) and one polynaftalene-based (PNS) superplasticizer. The dosage of the admixture in the paste was varied to assure a mini-slump flow diameter of 300 ± 10 mm. The PCE dispersant was retained for the concrete evaluation.

3.1.4 Aggregates

Missouri river sand and two crushed limestones, with nominal maximum aggregate sizes of 19.0 and 9.5 mm were used for the concrete study. The sand had a density of 2610 kg/m^3 and an absorption of 0.37%. The smaller and large coarse aggregate had a density of 2780 kg/m^3 and 2740 kg/m^3, respectively. The absorption values for the aggregates were 0.46% and 0.70%, respectively.

3.2 Mix design and mixing procedure for cement pastes

The investigation on the cement pastes was divided into two subtasks. For both dispersing admixtures, the influence of w/c was evaluated, in absence of any SCM or filler. Consecutively, the PCE dispersant and a w/cm = 0.35 was retained for the investigation on the SCMs and fillers.

3.2.1 Mixing procedure

All mixtures were prepared in a small Hobart mixer. Table 2 shows the different steps in the procedure, in which mixing and scraping are altered to ensure the homogeneity of the sample. The contact time between cement and water is taken as the reference time. The starting time of the rheological measurements is relative to this reference time. The dispersing admixture (SP) is added in delayed fashion. The desired quantity is determined through preliminary tests, evaluating the mini-slump flow for different dosages.

3.2.2 Mix design

Table 3 represents the mix designs evaluated. All cement pastes were prepared in a small Hobart mixer. The volume of cement paste produced is 750 ml for each mixture.

Table 2. Mixing procedure for cement pastes.

TIME	DURATION	ACTION	ADDITION
-0.5 min	30 s	Mixing	Dry materials
0 min	60 s	Mixing	Water
1 min	60 s	Scraping	
2 min	30 s	Mixing	
2.5 min	120 s	Mixing	SP
4.5 min	30 s	Scraping	
5 min	60 s	Mixing	

Table 3. Mix designs of investigated cement pastes (in grams for 750 ml of paste)

	CEMENT	WATER	SCM	DISPERSANT	W/CM
PCE 0.30	1218	365		PCE: 4.4	0.30
PCE 0.35	1126	394		PCE: 3.0	0.35
PCE 0.40	1048	419		PCE: 2.0	0.40
PCE 0.45	979	441		PCE: 1.5	0.45
PNS 0.30	1218	365		PNS: 12.2	0.30
PNS 0.35	1126	394		PNS: 8.8	0.35
PNS 0.40	1048	419		PNS: 4.1	0.40
PNS 0.45	979	441		PNS: 2.2	0.45
SLAG 25	845	394	Slag: 282	PCE: 2.6	0.35
LF 10	1014	394	Limestone: 113	PCE: 2.8	0.35
SF 5	1070	394	Silica fume: 56	PCE: 4.9	0.35
MK 25	845	394	Metakaolin: 282	PCE: 11.2	0.35
KA 1	1115	394	Kaolin: 11	PCE: 3.6	0.35
NS 1	1115	394	Nanosilica: 11	PCE: 6.1	0.35
AC 0.5	1121	394	Attapulgite clay*[2]: 6	PCE: 10.7	0.35
SL 25 – SF 5	789	394	Slag: 282 Silica fume: 56	PCE: 4.0	0.35
SL 25 – AC 0.5	839	394	Slag: 282 Attapulgite clay: 6	PCE: 9.8	0.35
SF 5 – AC 0.5	1064	394	Silica fume: 56 Attapulgite clay: 6	PCE: 23.3	0.35
SL 25 – SF 5 – AC 0.5	783	394	Slag: 282 Silica fume: 56 Attapulgite clay: 6	PCE: 14.9	0.35

[2] *It should be noted that the Attapulgite clay is delivered in slurry form. The reported values are the mass of active ingredient. The added water of the mixture has been compensated for the water in the slurry. The amount of water reported is the total amount of water in the cement paste.*

3.3 Mix design and mixing procedure for concrete

The concrete study was divided into two parts, investigating the effect of the differences in excess paste layer thickness, and a verification of the ideal combinations of supplementary cementitious materials, once the ideal excess paste layer thickness was known.

3.3.1 Determination of aggregate maximum packing density and excess paste layer thickness

The maximum packing density of the sand and coarse aggregates was determined using the gyratory intensive compaction tester (ICT). A dry homogenous mixture of coarse and fine aggregates was placed in the cylinder mold, rotating at a gyratory angle of 40 mrad for 124 cycles under a constant vertical pressure of 1.5 bar. Due to the gyratory inclination, shear movement under vertical pressure permits to attain a higher packing density. The packing density of granular materials or aggregates (φ) is calculated as shown in the following eqs. 9 and 10:

$$\varphi = \frac{\varrho_d}{\varrho_{dmax}} \quad \text{(Eq. 9)}$$

$$\varrho_{dmax} = \frac{1}{\frac{P_1}{\varrho_1}+\frac{P_2}{\varrho_2}+\frac{P_3}{\varrho_3}+\cdots} \quad \text{(Eq. 10)}$$

where: P_1, P_2, etc. are the weight percentages of the aggregates used in the mixture
ρ_1, ρ_2, etc. represent the relative density values of the different aggregates.

After a few trials, the selected vertical pressure was below a critical value which led to grinding or crushing of the particles. The critical pressure for the tested granular material was determined by observing the top surface of the cylinder mold after each trial. It can also be determined using the difference between its particle size distribution (PSD) before and after applying various pressures. Also, the number of cycles selected was based on when density reached its peak value and there was no considerable change on further increase in cycles.

Different combinations of sand and coarse aggregates were evaluated, attempting to approach the model grain-size distribution from the modified Andreasen and Andersen model, using a distribution modulus (q) of 0.29. The final aggregate selection yielded a maximum packing density of 0.79, when employing 50% sand, 21% crushed limestone with NMS = 9.5 mm and 29% crushed limestone with NMS = 19.0 mm. It should be noted that the combination of aggregates to reach this maximum packing density not only depends on their gradation, but also their shape, angularity and roughness.

Assuming all particles in the combined aggregate as spherical, concrete mixtures with different excess paste layer thicknesses were created. Based on the maximum packing density of the aggregate combination employed, a paste volume of 21% would yield zero excess paste layer thickness, and no flow. The additional paste amounts were calculated to obtain excess paste layer thicknesses on all aggregates of 25, 30 and 40 μm, resulting in different concrete mix designs.

3.3.2 Concrete mix designs for excess paste layer thickness investigation

Using the principles from the previous section, a series of mix designs were developed with varying excess paste layer thicknesses, for which the 40 μm excess paste layer thickness mixture was considered the reference. At first, for the subsequent mixtures with lower excess paste layer thicknesses, the amount of dispersing admixture was adjusted to obtain a slump flow of 500 ± 50 mm (-SF mixtures). Secondly, a new series was produced in which the ratio of dispersing admixture to cement and cementitious materials was kept constant. All mixtures were prepared with a w/cm (or w/b) equal to 0.35, using a binder combination of 95% Portland cement and 5% silica fume. The mixtures with constant dispersant dosage are labeled with "-SP" in Table 4. The number indicates the calculated excess paste thickness.

Table 4. Concrete mix designs with varying excess paste layer thickness. All units are in kg/m³ unless specified otherwise.

	CEM.	SILICA FUME	19 MM AGG.	9.5 MM AGG.	SAND	WATER	SP	W/B (-)
40-REF	455.0	23.9	517.8	369.9	884.2	166.5	1.66	0.35
30-SF	416.4	21.9	538.9	384.3	917.1	156.9	1.74	0.35
25-SF	396.0	20.8	550.2	392.6	936.5	149.4	2.15	0.35
25-SP	396.1	80.9	551.0	392.7	939.5	145.6	1.45	0.35
30-SP	416.5	21.9	539.6	384.6	920.1	153.0	1.52	0.35

3.3.3 Concrete mix designs for binder combination verification

As will be discussed in the results section, the ideal excess paste layer thickness was 40 µm. Five additional concrete mixtures were prepared attempting to guarantee fluidity while maximizing thixotropy. One of the main challenges was the influence of the dispersing admixture, opposing any factor which causes an increase in thixotropy but a decrease in fluidity. Binary mixtures with cement and slag cements A and B were produced, as well as ternary mixtures with cement, slag cements B and C and attapulgite clay. All mix designs are shown in Table 5.

Table 5. Mix designs for concrete mixtures for binder combination verification. All units are in kg/m³, unless specified otherwise.

	CEM	SLAG	AC	19 MM AGG.	9.5 MM AGG	SAND	WATER	SP	W/B (-)
SL-A	357.5	119.2	-	518.7	369.0	885.9	164.1	1.11	0.35
SL-B	355.6	118.5	-	518.7	369.0	885.9	163.2	1.11	0.35
SL-B-1	355.6	118.6		517.5	369.1	890.7	159.7	1.0	0.35
AC	478.3	-	2.4	517.5	369.1	890.7	159.8	2.7	0.35
SL-B-AC	352.2	118.2	2.4	517.1	369.2	898.1	150.4	3.0	0.35
SL-C-AC	350.8	117.7	2.4	519.0	369.8	906.3	138.8	3.83	0.33

3.3.4 Mixing procedure for concrete

All VFC mixtures were prepared in 75 l batches in a drum mixer with capacity of 150 l. Similar to the paste mixing procedure, the contact between water and binder is taken as the reference time. The elapsed times when executing green strength measurements and rheological measurements are relative to this reference time. The dispersing admixture (SP) is added in delayed fashion. The mixing procedure is conducted as shown in Table 6, and the slump flow test was carried out to check the acceptance criterion (500 ± 50 mm).

Table 6. Mixing procedure for concrete.

TIME (MIN)	DURATION	ACTION AND ADDITION
-1.00	1 min	Mix Aggregates + 1/2 water
0.00	30 sec	Add binders then add rest of water
0.50	1 min 30 sec	Mixing
2.00	1 min	Add SP
3.00	1 min	Rest and scraping
4.00	2 min	Mixing
6.00		Stop mixer
6.00	6 min	If slump flow 500 ± 50 mm achieved - Mixer agitated on slow speed and start testing at 15 min
		Else addition of SP and remixing

3.4 Rheological measurements on cement pastes

3.4.1 Measurement procedure

The rheological properties of the cement pastes were evaluated with the Anton Paar MCR 302, in parallel plate configuration. The plates are 50 mm in diameter and are sandblasted to minimize slip between the plates and the sample. The gap was maintained at 1 mm, and temperature was kept constant at 20°C. The temperature-controlling hood was placed on top of the system in an attempt to minimize the evaporation of water from the sample.

Immediately after mixing and the evaluation of the mini-slump flow, a small sample of cement paste is placed on the bottom plate. The lowering of the upper plate squeezes the sample in between both plates, filling up all space in between the plates. The edges of the plates were trimmed to avoid the edge effects.

The sample was evaluated using two different procedures: a flow curve, and static yield stress measurements at rest. The flow curve is measured by imposing a linearly decreasing shear rate with time, ranging from 100 s^{-1} to 5 s^{-1} in a 30 s timeframe (interval 2 in Figure 13). The flow curve is preceded by a 90 s pre-shear period, during which the shear rate is kept constant at 100 s^{-1} (interval 1 in Figure 13). This pre-shear is imposed to bring all samples to the same reference state (corresponding to this shear rate), in an attempt to eliminate the shear history (mixing, placing and rest) from the sample prior to the measurements. The flow curve is used to determine the dynamic yield stress and plastic viscosity (if the material obeys the Bingham model), or the modified Bingham model was imposed in case the sample was severely shear-thickening.

To determine the thixotropic properties, the sample was subjected to a constant shear rate of 0.005 s^{-1} (exaggerated in Figure 13). The corresponding shear stress evolution of the sample is monitored over a 60 s time period. When the thixotropic properties were evaluated immediately after obtaining the flow curve (interval 3 in Figure 13), a steady increase in shear stress is monitored. This increase in shear stress is a reflection of the thixotropic properties, immediately after mixing. This thixotropic measurement is then repeated four times at 5 minute intervals, each time giving the sample 4 min rest, while measuring the shear stress response in the 5^{th} minute (intervals 5, 7, 9 and 11 in Figure 13). For these profiles, as a larger static yield stress is developed, the shear stress shows, potentially, a steep slope with time, reaches a peak, followed by a descending curve. The first part of the curve corresponds to the elastic deformation, while the peak corresponds to the static yield stress: the stress needed to initiate flow after rest.

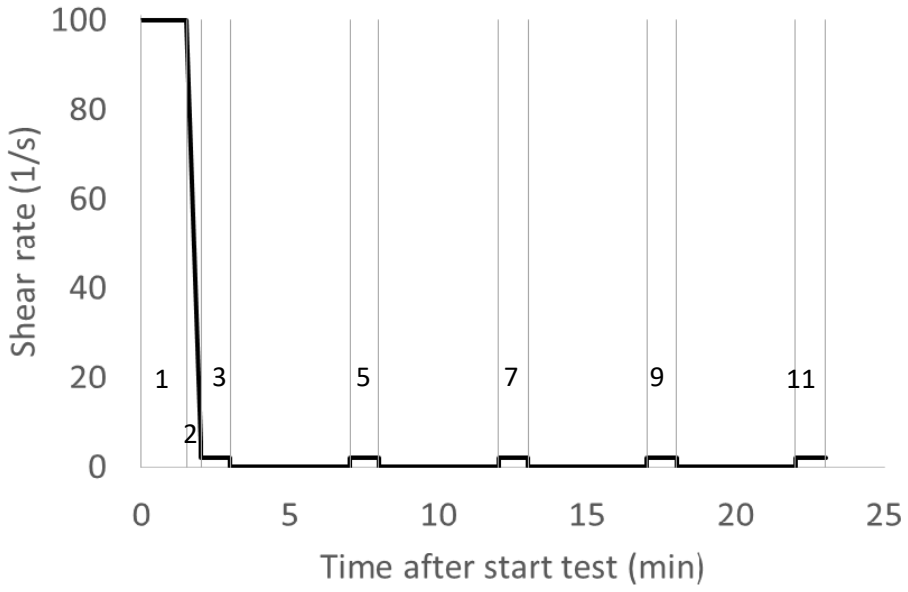

Figure 13. Shear rate profile. Interval 1 is the pre-shear, interval 2 represents the flow curve. During intervals 3, 5, 7, 9 and 11, the sample is sheared at 0.005 s^{-1} during 1 minute (the figure is exaggerated to enhance visibility). In between intervals 3, 5, 7, 9 and 11, the sample is at rest.

The pre-shear prior to the flow curve tests starts at 15 min after contact between water and cement. The first flow curve is determined between 16.5 and 17 min, and in the 17th, 22nd, 27th, 32nd and 37th minute, the stress response to a very small shear rate is determined. The entire procedure: pre-shear, flow curve and 5 thixotropy tests, is repeated on the same sample, 45 min after contact between cement and water. By comparing both flow curves at 15 and 45 min, an indication is given on the contribution of workability loss (mainly caused by strong C-S-H connections between the particles) to the stress development. For practical applications, the workability loss is less favorable in the case of prolonged transportation times.

3.4.2 Determination of rheological properties

Figure 14 shows a typical result of the flow curve measurement. The measured torque (T) is expressed as a function of the angular velocity (Ω). By means of a Reiner-Riwlin type of equation for parallel plate rheometers, the intercept of the T-Ω curve is transformed into the yield stress, and the slope of the curve can be used to calculate the viscosity. For the shown example, the yield stress is 5.1 Pa, and the plastic viscosity is 0.72 Pa s at 15 min. The evolution of the obtained (dynamic) yield stress from 15 to 45 min is used to evaluate the workability loss of the mixture.

Figure 15 shows the typical stress response at a constant shear rate of 0.005 s^{-1}, immediately measured after the flow curve. In total, 100 data points are determined in 60 s. The shear stress profile shows a continuously increasing shear stress with time, attributed to the restructuring of the material under very small shear. The average of the last 20 data points is taken as one of the parameters studied: it indicates how much yield stress the sample can develop immediately after shearing.

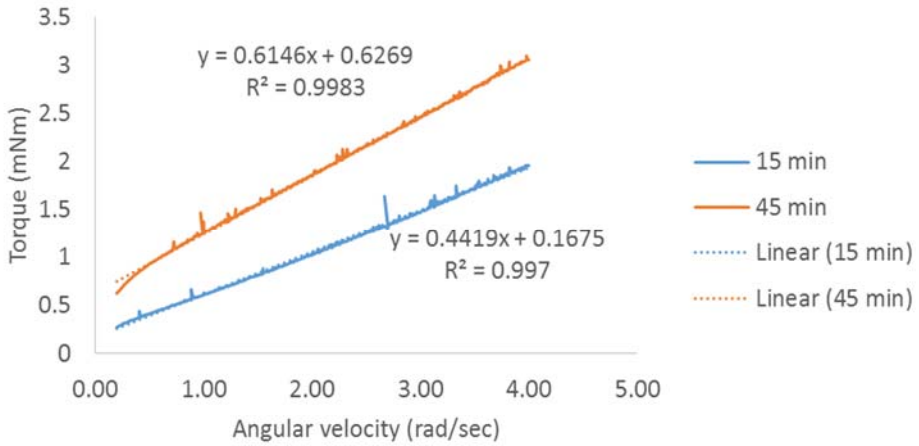

Figure 14. Flow curves at 15 and 45 min for the PCE 0.35 mixture.

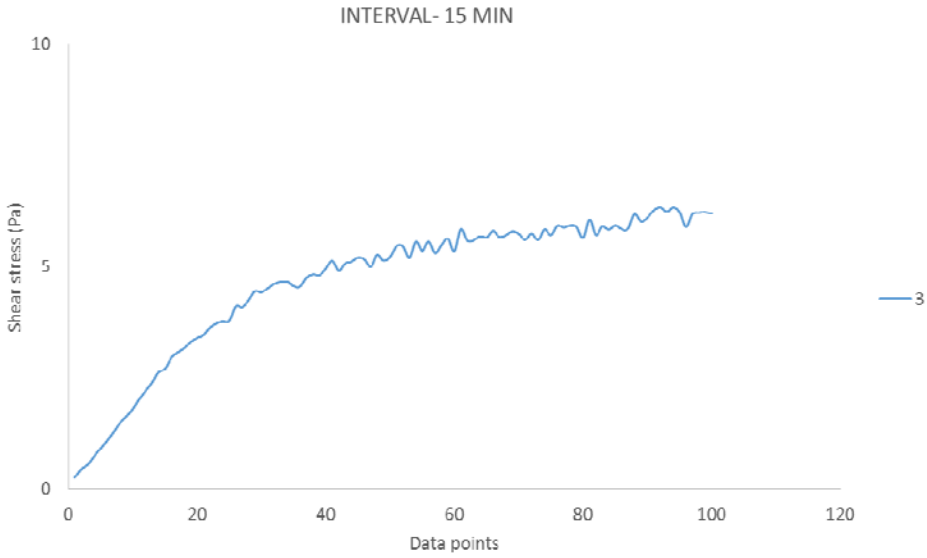

Figure 15. Typical result of the increase in shear stress at a constant shear rate of 0.005 s^{-1}, immediately after obtaining the flow curve. Result shown is for the PCE 0.35 mixture at 17 min.

Figure 16 shows the remaining static yield stress responses. The legend indicates the measurement intervals in the rheometer. For intervals 5, 7, 9 and 11, the maximum values are considered the static yield stress. The thixotropy is further evaluated by the average increase in static yield stress with time ($\Delta\tau_{0,s}$: static yield stress minus shear stress at end of interval 3 / elapsed time since the end of the flow curve), as well as the individual value of the 5th interval, corresponding to a 5 min rest (in fact, 1 min at 0.005 s^{-1}: interval 3, and 4 min rest).

$$\Delta\tau_{0,s} = \frac{\tau_{0,s,x} - \tau_{0,s,3}}{t_x - t_3} \qquad \text{(Eq. 11)}$$

Where: $\Delta\tau_{0,s}$ = the increase of static yield stress (Pa/min)
$\tau_{0,s,x}$ = the static yield stress measured in interval x (Pa) (x = 5, 7, 9, or 11)
t_x = time at which $\tau_{0,s,x}$ is measured

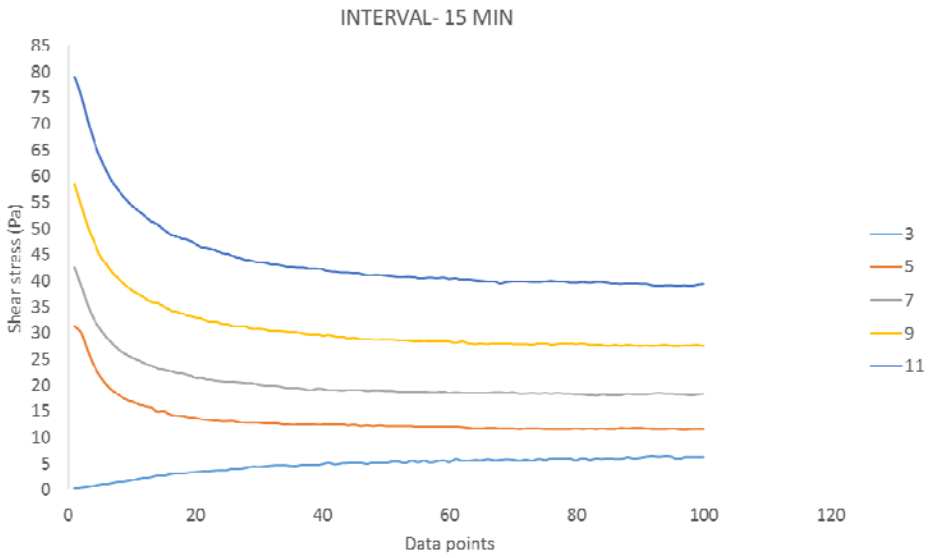

Figure 16. Static yield stress measurements. The colors represent the measurement intervals in the rheometer. Results for the PCE 0.35 mixture at 15 min.

To summarize: the following parameters are used for the evaluation of the rheological properties:

- Increase in dynamic yield stress, obtained from the flow curves between 15 and 45 min, to determine the workability loss.
- The average shear stress at the end of the third interval, just after the flow curve, which corresponds to the immediate development of internal structure.
- The increase in static yield stress over 5 min of rest, taken as the maximum shear stress value at interval 5 minus the value at the end of interval 3.
- The average increase in static yield stress with time, taken as the average of the maximum shear stress (minus shear stress at the end of interval 3) divided by the elapsed time since the end of the flow curve, for intervals 5, 7, 9 and 11.

3.5 Rheological measurements on concrete

The rheological measurements on concrete were executed with an ICAR rheometer. This device consists of a 4-blade vane with a radius of 63.5 mm and a height of 127 mm. The bucket of the reservoir has a radius of 143 mm, able to accommodate aggregate sizes up to 20 mm, according to the developers. Two testing procedures were executed on the concrete: a dynamic test and a static test. Both testing procedures were executed twice: once after mixing at 15 min after contact between cement and water, and second time at 70 ± 10 min after cement-water contact. Just before sampling the concrete for the second set of measurements, the mixture was intensely mixed in the drum mixer to mimic concrete arriving on a jobsite.

3.5.1 Dynamic rheology tests

Prior to mixing, an empty test was executed to correct for slightly negative torque values during rotation. Immediately after mixing, freshly mixed concrete was placed in the rheometer container while the impeller remained inserted in the concrete. At 15 min after contact between cement and water, a pre-shear period was imposed for 20 seconds at a rotational velocity of 0.50 rps to eliminate the shear history from the sample prior to measuring. During this process, the torque gradually declines till it reaches equilibrium. This

represents the amount of energy required to break down the internal structure of concrete mixture. After the pre-shear, the flow curve was measured by decreasing the rotational velocity stepwise from 0.5 to 0.03 rps in 10 steps of 5 s each. The flow curve was used to determine the dynamic yield stress and plastic viscosity using the Bingham model. Based on the measured torque-time profile, points which did not show equilibrium, or showed extreme scattering were discarded. The remaining torque data were averaged at each rotational velocity step, and the corresponding zero-value was subtracted. The relationship between the obtained corrected torque (T) and the rotational velocity (N) was fitted linearly, from which the yield stress and plastic viscosity can be determined using the Reiner-Riwlin equation. Plug flow was verified by comparing the stress at the outer radius of the rheometer to the yield stress. If necessary, an iterative procedure was employed, reducing the flow domain to the sheared area, to recalculate the rheological properties [31].

3.5.2 Static rheology tests

After the flow curve, the top of the rheometer was removed from the container and the sample was re-homogenized by hand prior to the thixotropic measurements. To measure the thixotropic properties, a rotational velocity of 0.003 rps was imposed on the sample at rest and a steady increase in torque was monitored. The test was terminated after a peak in torque was achieved. The maximum torque value can be related to the stress required to initiate the flow after rest.

The stress growth or thixotropy test was measured four times, i.e., the measurements were conducted at resting periods of 3 min (i.e. 22nd min from water-binder contact), 5 min, 8 min, and 15 min, respectively. For example, the sample is at rest for 5 min between the 1st and 2nd measurement. After the four static yield stress measurements, the sample was then returned to the mixer and agitated (slow speed). Before the second series of measurements (flow curve + 4 static yield stresses), the speed of mixer is increased to simulate the re-mixing process of a truck mixer before the placement process on site. The entire procedure was repeated and thixotropy measurements were conducted in a similar fashion. The flow curve and stress growth results obtained after 1st and 2nd measurements were compared to determine the workability loss in concrete and its influence on the thixotropic properties.

The stress growth measurements were conducted at four different intervals. The corrected maximum torque value with the zero measurement, was then transformed to measure the static yield stress by the following equation (Eq. 12):

$$\tau_{0,s} = \frac{T_{max}}{2\pi R_i^2 h} \quad \text{(Eq. 12)}$$

Figure 17 shows the typical stress response where intervals 1, 2, 3, and 4 represent the stress measurements at resting periods of 3 min, 5 min, 8 min, and 15 min; i.e. 22nd, 27th, 35th, and 50th min from the water-binder contact. Similar to the cement paste study, the thixotropy is further evaluated by the average increase in static yield stress with time ($\Delta\tau_{0,s}$: static yield stress minus shear stress at end of interval 1 / elapsed time between two yield stress measurements (see Eq. 11, but taking t_1 as reference time)).

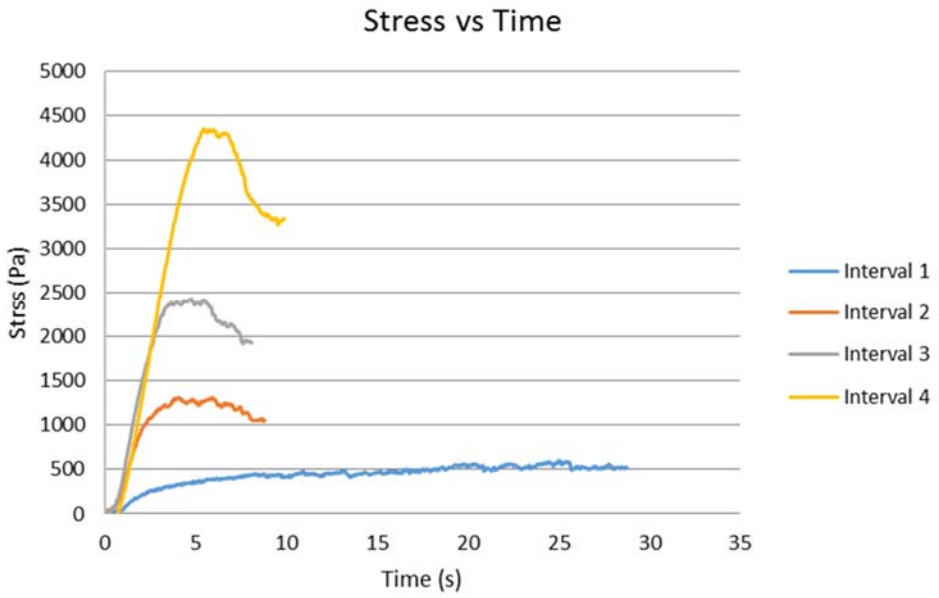

Figure 17. Typical example of stress growth test results.

3.6 Other workability tests on concrete

Apart from flow curve measurements and static yield stress tests on fresh concrete, two other tests were employed to evaluate the flowability of the concrete and the development of the green strength. Similarly as for the rheology tests, all tests were executed in two sequences: once at 15 min after cement-water contact and a second round at 70 ± 10 min.

3.6.1 Slump flow test

The slump test was carried out according to ASTM C1611-14. This test is specified for SCC mixtures in which a sample of freshly mixed concrete is placed in the Abram's cone in one layer on a flat, level, and nonabsorbent surface without any tamping or vibration. The cone was then raised in 3 ± 1 s and the average of two orthogonal diameters of the concrete spread was measured. After removal of the mold, the time required to reach 50 cm circle was measured to determine the T50 of the mixture. A longer T50 time represents higher viscosity. The slump flow test, including T50, was repeated around 75 min from the water-binder contact. The change in slump flow indicates the workability loss of the VFC mixture.

3.6.2 Density and fresh concrete air content

The density of freshly mixed concrete was determined according to ASTM C 138-08. A sample of freshly mixed concrete was placed without any rodding or vibration in a measuring bowl conforming to ASTM C 231. A strike-off bar was used to remove top surface of concrete and finished it smoothly. The same mixture was also used to determine the air content by pressure method, using type B-meter, according to ASTM 231-14.

3.6.3 Green strength test

To evaluate the green strength development of the VFC mixtures, removable cylindrical metal molds of 100 mm in diameter and 200 mm in height were used for concrete casting (Figure 18 (a)). On a flat surface, the two semi-cylinder molds were clamped together, standing on a nonabsorbent metal plate (Figure 18 (b)). During casting, freshly mixed concrete was placed in the cylinder in two layers without any vibration or rodding. After each layer, the mold was gently tapped to remove entrapped air. The cylinders were cast in a

sequence of the testing protocol and remained undisturbed during the resting time. Each cylinder mold was removed at a given time and a cylinder with good shape stability, i.e. with slightly or no deformation, was further tested for green strength as shown in Figure 18 (c). A square shaped plate was placed on top of the cylinder, guided by two vertical rods, and the cylinder was loaded with standard load blocks until collapse as shown in Figure 18 (d). The total weight of load applied during the test divided by the loading area provides the green strength of concrete mixture.

During casting, freshly mixed concrete was filled in four molds and the same sequence was followed for the green strength measurement to study the development of shape stability with time. The first cylinder was demolded after a resting time (sample remains undisturbed) of 5 min, and similarly, the 2nd, 3rd, and 4th cylinder were demolded after a resting period of 9 min, 16 min, and 30 min, respectively. Before repeating the measurements at 70 min, the speed of the mixer is increased to simulate the re-mixing process of a truck mixer before discharging on site. The entire procedure was repeated and green strength tests were conducted on four molds at identical resting times.

(a) Removable 100 x 200 mm mold

(b) Mold clamped when placing concrete

(c) Typical shape-stable concrete

(d) Loading of samples using a square plate and different loads

Figure 18. Green strength test setup.

4 Results and Discussion

4.1 Measurements on cement paste

4.1.1 Influence of water-to-cement ratio and dispersant type

The influence of w/c and the dispersant type on the rheology, and in particular thixotropic build-up, has been investigated based on the first eight mixtures mentioned in Table 3. Table 7 shows the detailed results of all measurements. The first three columns represent the flow curve results, in terms of (dynamic) yield stress and viscosity, both at 15 and 45 min. The change in dynamic yield stress is an indication of the workability loss of the sample. The last three columns are reflecting the thixotropic build-up of the pastes. The static yield stress in interval 3 is measured during 1 min after the determination of the flow curve. The static yield stress increase with time in the following intervals is calculated by means of the $\Delta\tau_{0,s}$ equation (eq. 11).

The results in Table 7 and in Figure 19 to Figure 21 clearly show, as expected, that all rheological properties are directly dependent on w/c, regardless of the dispersant type. The lower w/c, the more thixotropic the mixtures are. An efficient way to increase thixotropy of cement pastes is to decrease w/c, especially for values of w/c below 0.40. In fact, at w/c = 0.40, no significant thixotropy in the pastes has been noticed. Regarding the dispersant type, the PNS superplasticizer delivers the largest increase in static yield stress in the first minute (Figure 20), but in the longer term, the increase in static yield stress for the PNS is lower than that for the PCE (Table 7, Figure 21).

Furthermore, the mixtures with PNS show a larger workability loss, based on the dynamic yield stress obtained from the flow curves (Figure 19). This is also reflected in a larger static yield stress value for the second measurement (starting at 45 min), compared to the first measurement (starting at 15 min). In case a long workability retention is desired (e.g. in case of long transportation times), this workability loss is disadvantageous. To reduce the workability loss, the PCE dispersing agent is selected for the next series of experiments. As thixotropy is largely dependent on w/c, the most logical choice to maximize thixotropy would be w/c = 0.30. However, detailed analysis of the static yield stress curves learns that the static yield stress does not substantially increase beyond 5 min of rest for the mixtures with w/c = 0.30. It appears that the static yield stress plateaus and any subsequent increase, especially for the measurements after 45 min, could be attributed to the hydration mechanism. This reduction in static yield stress can be clearly observed when comparing the last three columns in Table 7. The average increase in static yield stress over 20 min is approximately 65% smaller compared to the increase in the first minute for the PCE 0.30 system. The difference between the average increase in static yield stress and the increase in static yield stress in the first minute is less than 50% for the PCE 0.35 mixture, indicating a more prolonged increase in thixotropic properties (and hydration). The mixture with w/c = 0.35 also has a lower workability loss, and therefore, the PCE 0.35 mixture is selected as reference for the remaining part of the work on cement-pastes.

Table 7. Rheological results for the pastes with different w/c and different dispersant type. Note that YS stands for the yield stress, visco is the viscosity, ΔYS is the change in dynamic yield stress between the 15 and 45 min flow curve measurements. The static yield stress in interval 3 is the increase in shear stress (at 0.005 s^{-1}) during 1 minute immediately after determining the flow curve. The static yield stress in interval 5 stands for the increase in yield stress since interval 3, divided by the elapsed time. The average static yield stress increase stands for the evolution of static yield stress over intervals 5, 7, 9, and 11 (i.e. average static yield stress increase over 20 min).

	DYNAMIC YS (PA)	**VISCO (PA S)**	**ΔYS (PA/MIN)**	**STATIC YS INTERVAL 3 (PA/MIN)**	**STATIC YS INTERVAL 5 (PA/MIN)**	**AVERAGE STATIC YS (PA/MIN)**
PCE 0.30	*15'*: 8.1 *45'*: 30.7	*15'*: 1.01 *45'*: 1.40	0.76	*15'*: 20.0 *45'*: 53.0	*15'*: 11.6 *45'*: 15.2	*15'*: 6.4 *45'*: 8.7
PCE 0.35	*15'*: 5.1 *45'*: 19.2	*15'*: 0.72 *45'*: 1.00	0.47	*15'*: 6.2 *45'*: 22.4	*15'*: 5.0 *45'*: 12.0	*15'*: 3.9 *45'*: 7.2
PCE 0.40	*15'*: 2.4 *45'*: 7.4	*15'*: 0.25 *45'*: 0.38	0.17	*15'*: 0.5 *45'*: 3.6	*15'*: 0.7 *45'*: 3.1	*15'*: 1.2 *45'*: 2.9
PCE 0.45	*15'*: 2.9 *45'*: 6.5	*15'*: 0.13 *45'*: 0.20	0.12	*15'*: 0.9 *45'*: 2.5	*15'*: 1.1 *45'*: 1.7	*15'*: 1.0 *45'*: 1.5
PNS 0.30	*15'*: 12.3 *45'*: 40.7	*15'*: 0.90 *45'*: 1.14	0.95	*15'*: 20.4 *45'*: 60.4	*15'*: 7.2 *45'*: 13.5	*15'*: 4.1 *45'*: 8.2
PNS 0.35	*15'*: 13.3 *45'*: 37.0	*15'*: 0.25 *45'*: 0.36	0.79	*15'*: 10.7 *45'*: 42.7	*15'*: 2.1 *45'*: 11.6	*15'*: 2.2 *45'*: 7.5
PNS 0.40	*15'*: 6.3 *45'*: 14.5	*15'*: 0.17 *45'*: 0.26	0.27	*15'*: 0.3 *45'*: 4.8	*15'*: 0.1 *45'*: -	*15'*: 0.2 *45'*: 0.9
PNS 0.45	*15'*: 0.3 *45'*: 0.8	*15'*: 0.05 *45'*: 0.06	0.02	*15'*: 0.1 *45'*: 0.0	*15'*: 0.1 *45'*: 0.0	*15'*: 0.1 *45'*: 0.0

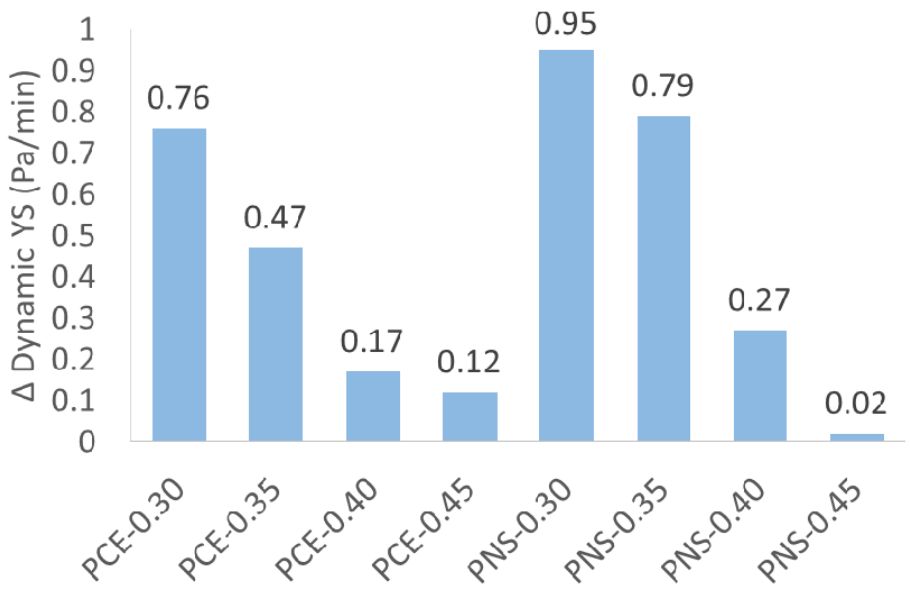

Figure 19. Increase in dynamic yield stress.

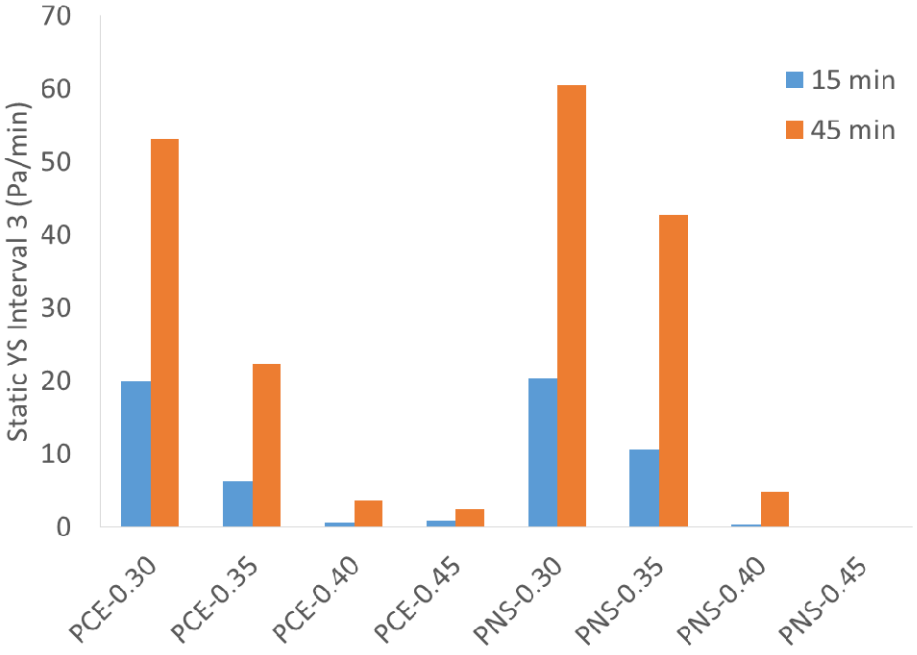

Figure 20. Static yield stress for interval 3.

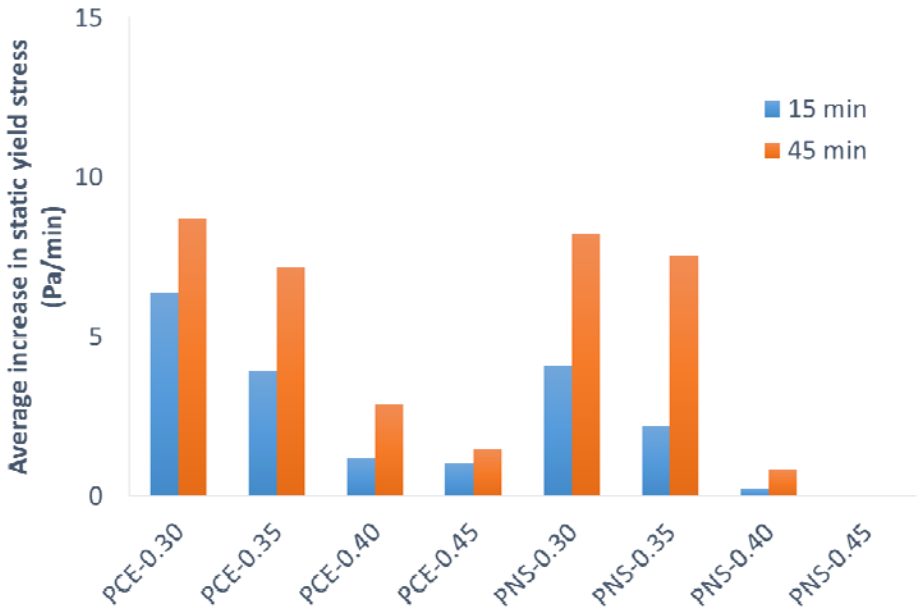

Figure 21. Average increase in static yield stress.

4.1.2 Influence of supplementary cementitious materials and mineral fillers

4.1.2.1 Binary binder systems

After the selection of the PCE dispersant and the 0.35 water-to-cement ratio, a number of different supplementary cementitious materials (SCMs) and mineral fillers were evaluated. Detailed results are presented in Table 8, and in Figure 22 to Figure 24. Figure 25 shows the SP consumption to reach the desired mini-slump flow (as reported in Table 3). From Figure 22, it can be seen that nearly all added SCMs or fillers cause a less important increase in dynamic yield stress compared to the reference mixture, except for the mixture with slag. It is also noteworthy to state that the mixture with 0.5% attapulgite clay showed no increase in dynamic yield stress and a slight increase in plastic viscosity. Comparing the increase in static yield stress during the 1st minute for the 15 min test, the reference mixture with plain OPC showed the largest increase, while the mixtures with attapulgite clay, silica fume and slag showed similar behavior (Figure 23). Limestone filler and metakaolin, at the used dosages, significantly reduce the thixotropic build-up.

However, the difference between the static yield stress at 15 min and the one at 45 min is largely influenced by the workability loss, as for the highly restructuring mixtures (REF, SL 25, SF 5 and AC 0.5), a direct relationship between the increase in dynamic yields stress from 15 to 45 min, and the static yield stress at 45 min can be found. From the average increase in static yield stress (Figure 24), for the test started at 15 min, the silica fume mixture shows the most important increase in static yield stress (considering that the results on the slag mixture were deemed erroneous). The mixtures with metakaolin and nanosilica also show a substantial increase in static yield stress, but the speed of development in the first minute was lower than the other mixtures. The attapulgite clay mixture shows a large increase in static yield stress in the first minute, but the increase in yield stress slows down over time.

Based on the above observations, silica fume, slag and attapulgite clay are retained for further analysis. Silica fume is a performance-enhancing SCM. It can reduce viscosity at a low dose and increases the thixotropic response of the mixture and reduces the workability loss, potentially due to the larger SP amount. The attapulgite clay is mostly beneficial for the immediate development of yield stress, but it requires a significant addition of dispersant, potentially causing the negligible workability loss. Slag shows a quick increase in

static yield stress, but causes a large workability loss, rendering the cement-slag combination on its own less favorable for potential extended transportation of the mixture.

Table 8. Rheological properties of cement pastes with binary composition (cement + 1 SCM or filler)

	DYNAMIC YS (PA)	VISCO (PA S)	ΔYS (PA/MIN)	STATIC YS INTERVAL 3 (PA/MIN)	STATIC YS INTERVAL 5 (PA/MIN)	AVERAGE STATIC YS (PA/MIN)
REF	*15'*: 5.1 *45'*: 19.2	*15'*: 0.72 *45'*: 1.00	0.47	*15'*: 6.2 *45'*: 22.4	*15'*: 5.0 *45'*: 12.0	*15'*: 3.9 *45'*: 7.2
LF 10	*15'*: 1.9 *45'*: 8.6	*15'*: 0.40 *45'*: 0.58	0.22	*15'*: 0.9 *45'*: 4.7	*15'*: 0.9 *45'*: 3.6	*15'*: 1.2 *45'*: 3.5
SL 25	*15'*: 6.2 *45'*: 22.4	*15'*: 0.46 *45'*: 0.78	0.54	*15'*: 4.8 *45'*: 24.6	*15'*: 5.3 *45'*: 13.5	*15'*: - *45'*: 9.2
SF 5	*15'*: 1.7 *45'*: 5.5	*15'*: 0.43 *45'*: 0.57	0.13	*15'*: 5.0 *45'*: 10.8	*15'*: 4.5 *45'*: 8.4	*15'*: 4.8 *45'*: 7.8
MK 25	*15'*: 2.2 *45'*: 3.8	*15'*: 0.59[3] *45'*: 0.77[3]	0.07	*15'*: 2.5 *45'*: 6.3	*15'*: - *45'*: 6.2	*15'*: 3.0 *45'*: 12.4
K 1	*15'*: 3.9 *45'*: 11.8	*15'*: 0.32 *45'*: 0.46	0.26	*15'*: 3.3 *45'*: 12.0	*15'*: - *45'*: 6.7	*15'*: 1.7 *45'*: 5.9
NS 1	*15'*: 1.3 *45'*: 7.0	*15'*: 0.39 *45'*: 0.61	0.19	*15'*: 3.9 *45'*: 12.9	*15'*: 2.6 *45'*: 8.9	*15'*: 3.2 *45'*: 8.1
AC 0.5	*15'*: 1.5 *45'*: 1.6	*15'*: 0.27 *45'*: 0.38	0.00	*15'*: 5.3 *45'*: 6.2	*15'*: 2.2 *45'*: 2.4	*15'*: 1.5 *45'*: 2.4

[3] *The metakaolin mixture showed severe shear-thickening behavior, and the viscosity was approximated as the differential viscosity at 50 s^{-1}.*

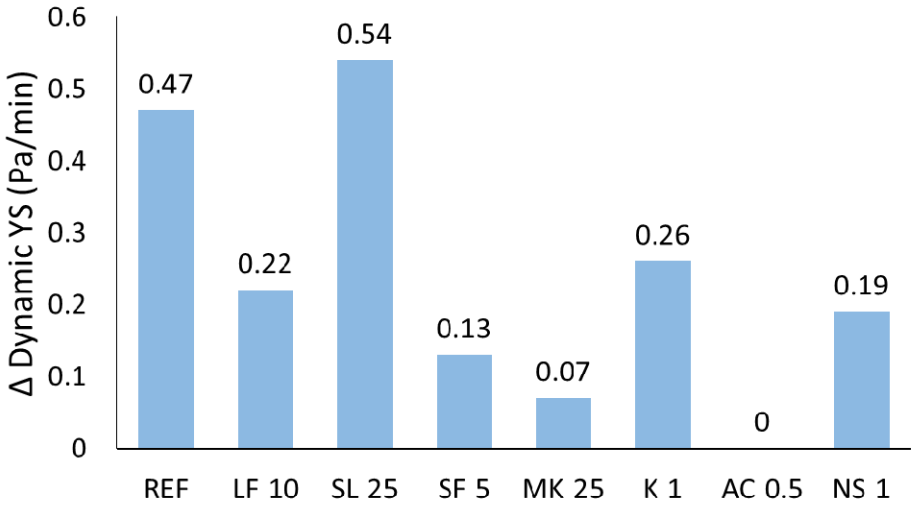

Figure 22. Increase in dynamic yield stress of binary systems.

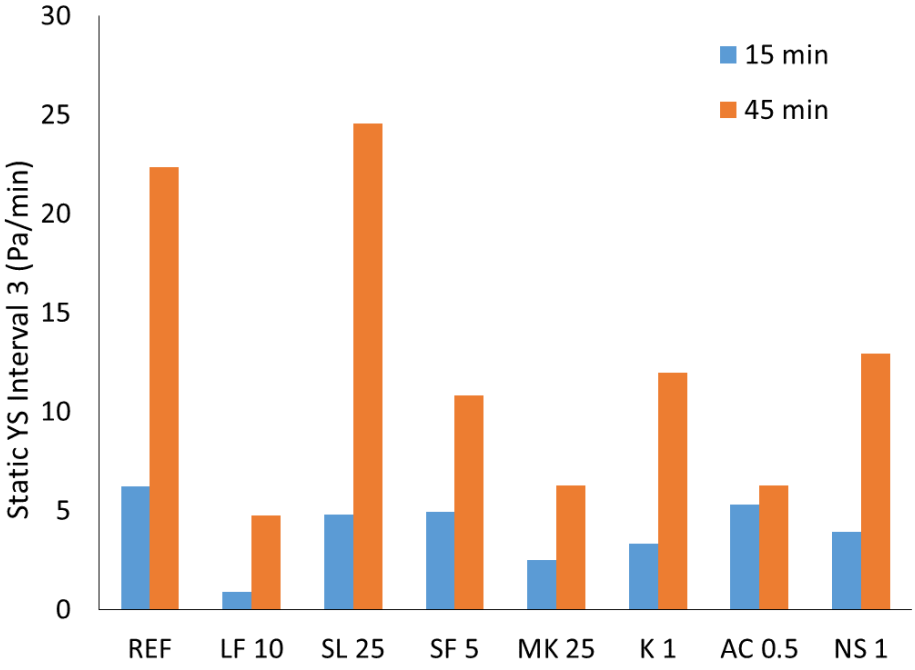

Figure 23. Static yield stress in interval 3 for binary systems.

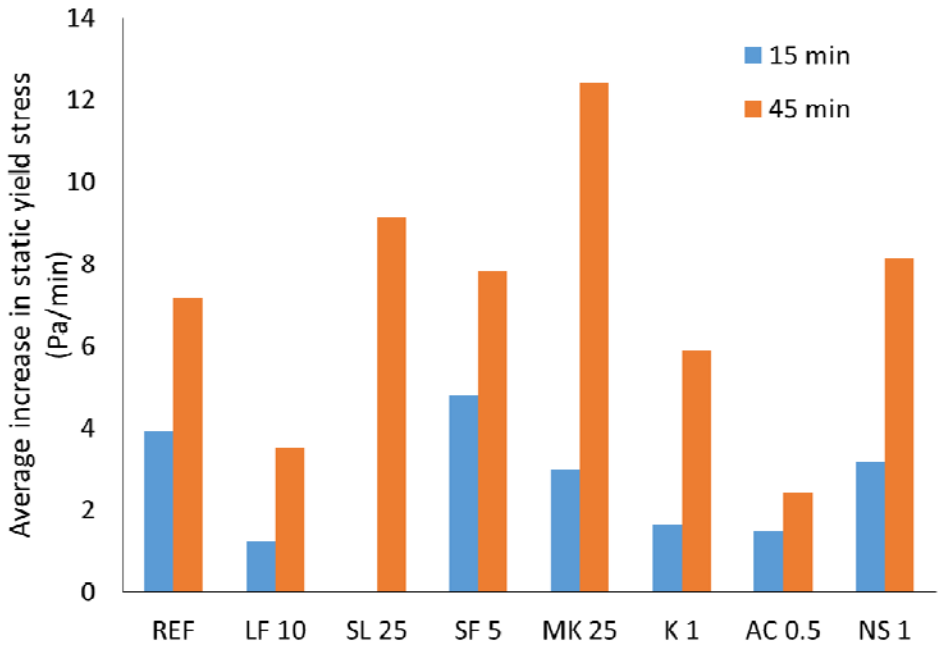

Figure 24. Average increase in static yield stress for binary systems.

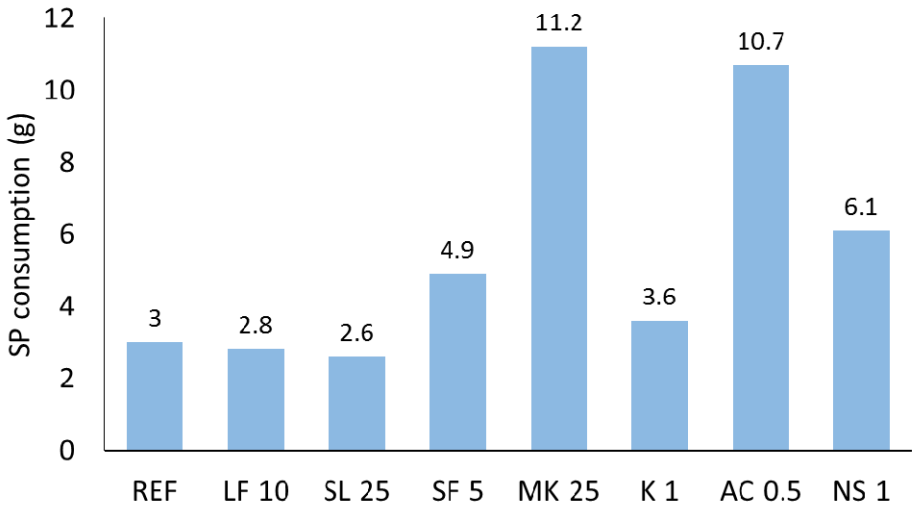

Figure 25. SP consumption of binary mixtures.

4.1.2.2 Ternary and quaternary binder systems

When starting the subtask on ternary binder systems, a new delivery of cement was made to the laboratory. Although the cement is the same type, produced by the same producer as the previous delivery, some changes in physical properties and chemical composition may affect the rheological response of the mixtures. Therefore, the reference mixture with no SCMs or binders, a w/c = 0.35 and the PCE dispersing admixture, was reproduced and the new values of the rheological properties are reported in Table 9. It should also be noted that the SP quantity necessary to achieve a mini-slump flow of 300 ± 15 mm was slightly lower: 2.9 g for the new cement relative to 3.0 g for the old delivery.

The results for the ternary and quaternary mixtures are summarized in Table 9. In Figure 26 to Figure 28, the rheological properties of the ternary and quaternary mixtures are shown. The new reference cement mixture and the binary systems with slag, silica fume and attapulgite clay are also included in the figures to enhance visual assessment. Figure 29 shows the SP demand of the studied binder systems. The increase in dynamic yield stress from 15 to 45 min is substantially lower for all mixtures containing attapulgite clay, despite the inclusion of slag in some of the mixtures. This can most likely be attributed to the increased SP dosage, as the dosage is at least of the same magnitude as the binary mixture with attapulgite clay. The ternary mixture with slag and silica fume shows a workability loss in between that of the binary mixtures with slag and silica fume separately.

Table 9. Rheological properties of ternary and quaternary systems.

	DYNAMIC YS (PA)	VISCO (PA S)	ΔYS (PA/MIN)	STATIC YS INTERVAL 3 (PA/MIN)	STATIC YS INTERVAL 5 (PA/MIN)	AVERAGE STATIC YS (PA/MIN)
REF-NEW	*15'*: 11.0 *45'*: 27.9	*15'*: 0.34 *45'*: 0.53	0.56	*15'*: 5.3 *45'*: 23.3	*15'*: 0.6 *45'*: 7.8	*15'*: 3.9 *45'*: 7.2
SL 25 – AC 0.5	*15'*: 6.7 *45'*: 7.7	*15'*: 0.33 *45'*: 0.44	0.03	*15'*: 18.9 *45'*: 22.4	*15'*: 8.3 *45'*: 8.6	*15'*: 7.8 *45'*: 7.7
SF 5 – AC 0.5	*15'*: 10.5 *45'*: 10.7	*15'*: 0.47 *45'*: 0.53	0.01	*15'*: 6.9 *45'*: 7.7	*15'*: 1.8 *45'*: 1.8	*15'*: 1.2 *45'*: 1.3
SL 25 – SF 5 – AC 0.5	*15'*: 3.6 *45'*: 4.0	*15'*: 0.29 *45'*: 0.36	0.02	*15'*: 6.7 *45'*: 7.4	*15'*: 3.5 *45'*: 3.4	*15'*: 2.7 *45'*: 2.8
SL 25 – SF 5	*15'*: 7.8 *45'*: 16.8	*15'*: 0.37 *45'*: 0.50	0.30	*15'*: 12.5 *45'*: 23.3	*15'*: 4.2 *45'*: 10.9	*15'*: 4.1 *45'*: 8.6

The increase in static yield stress within the first minute (interval 3), is for all ternary and quaternary mixtures higher than for the reference and binary mixtures. However, the benefit of combining attapulgite clay and silica fume is only minor and a significant increase in SP consumption is noted, making these mixtures less favorable. The mixture with slag and attapulgite clay shows a strong increase in thixotropic capacity, without showing a substantial loss in workability. Combining slag and silica fume also delivers a significant increase in static yield stress development, but the workability loss may affect the results. The average increase in static yield stress shows similar behavior: combining silica fume and attapulgite clay, with or without slag, results in inferior rheological response compared to only employing silica fume.

Based on all data shown, the following mixtures are deemed optimal for the further development of VFC for slipform applications:

- A ternary mixture combining 25% slag and 0.5% attapulgite clay, intended for extended transportation times, as the thixotropic build-up is significant and the workability loss is minor.
- A ternary mixture containing 25% slag and 5% silica fume, as an alternative if attapulgite clay is not available. This mixture also shows substantial thixotropic build-up, but the workability loss can be high. Hence, this mixture could be suitable for on-site or nearby concrete production and placement. A mixture with only 5% silica fume could work as an alternative. A binary mixture with only 25% slag is not recommended, as the workability loss is deemed to be the main mechanism for

the static yield stress development. Non-reversible build-up of yield stress could limit self-consolidation if the waiting time is too elevated.

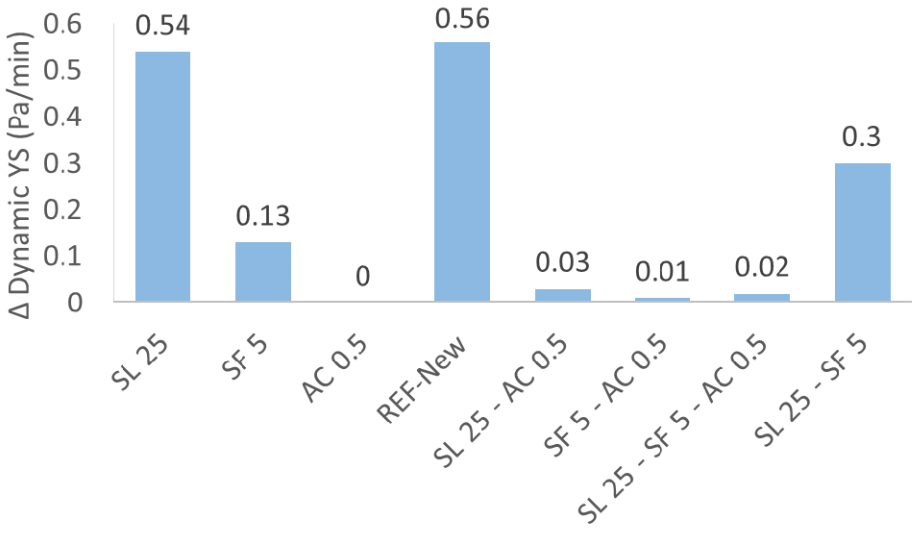

Figure 26. Increase in dynamic yield stress for ternary and quaternary systems.

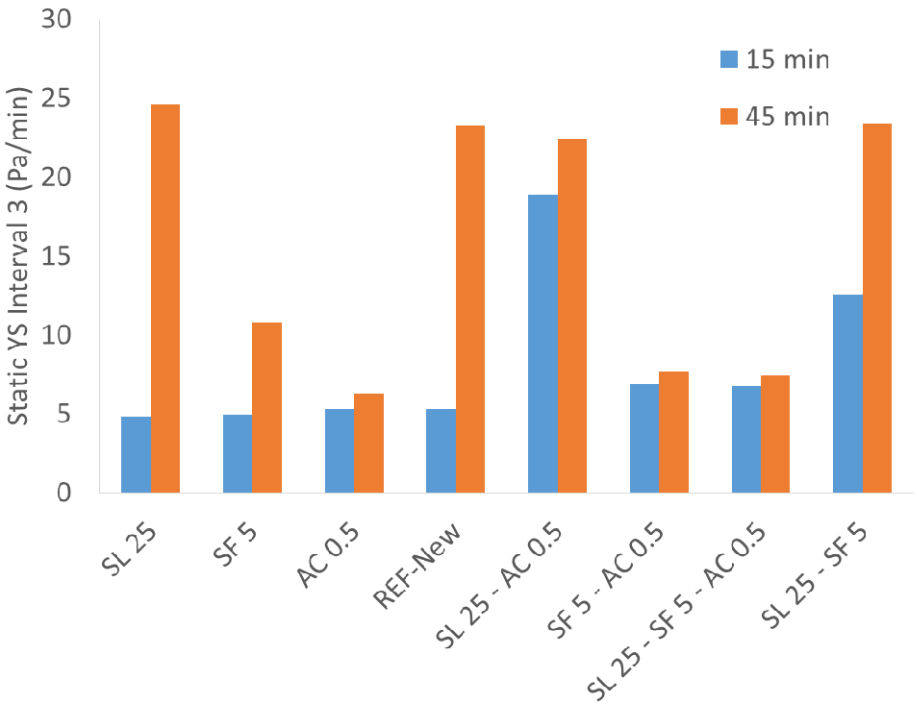

Figure 27. Static yield stress at the end of the 3rd measurement interval for ternary and quaternary systems.

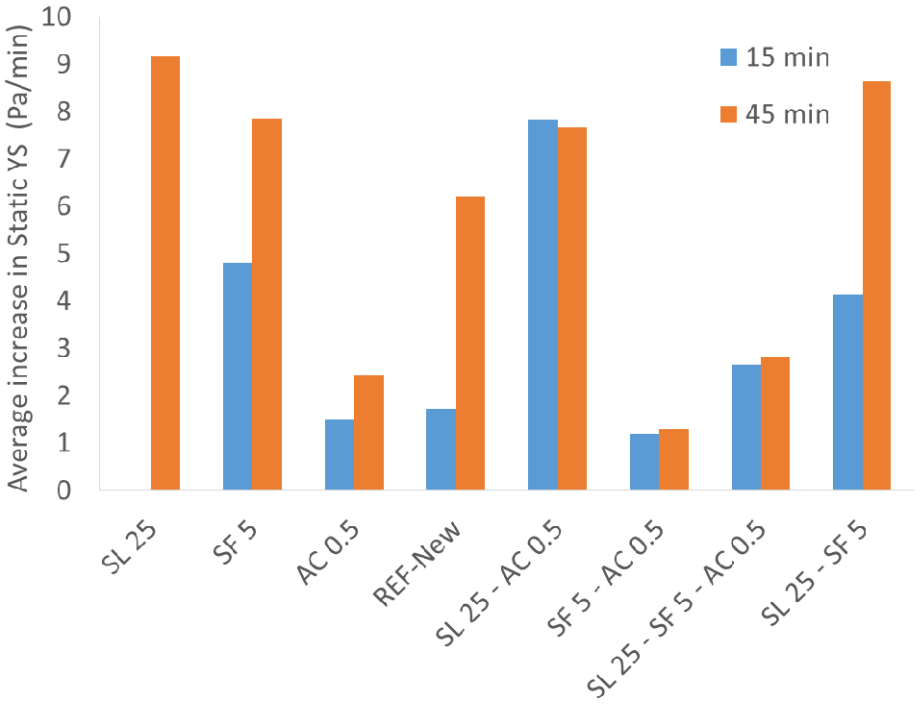

Figure 28. Average increase in static yield stress for ternary and quaternary systems.

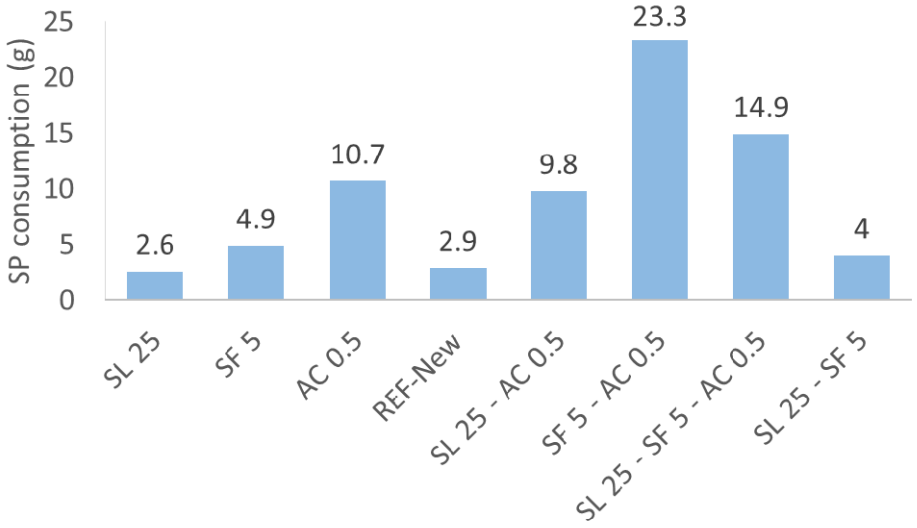

Figure 29. SP demand for ternary and quaternary systems.

4.1.3 Summary for measurements on cement pastes

Based on the measuring procedure for cement pastes, different parameters describing the evolution of rheological properties with time are derived: the increase in dynamic yield stress with time, reflecting workability loss; the increase in static yield stress immediately after determining the flow curve (interval 3) as a measure of instant build-up; and the average increase in static yield stress with time A_{thix}, showing the longer-term increase in stiffness of the pastes.

The results obtained for mixtures with different w/c follow the logical order, but the long-term gain in thixotropy (reflected by the average A_{thix} for the 15 and 45 min period) is not as substantial as expected for the w/c = 0.3 mixture, while it required a larger dosage of PCE and the workability loss was also larger. The PCE-based dispersing admixture seemed more beneficial in terms of workability retention and in thixotropy development.

For the binary binder systems, the largest immediate increases in static yield stress were obtained for the mixtures with slag, silica fume, attapulgite clay and the pure cement mixture. A_{thix}-values, measured over a more extended period were higher for the slag and silica fume mixtures, and for the metakaolin mixture at later age. Workability loss was almost non-existent for the attapulgite clay mixture, which is attributed to the high PCE dosage.

Based on the best-performing types of supplementary cementitious materials, ternary and quaternary binder systems were evaluated. The most remarkable result is combinations of attapulgite clay and silica fume only improve immediate yield stress development, but the long-term development is strongly reduced when using those materials combined. The workability loss in those combinations is also close to zero, and those mixtures require a large dosage of the dispersing admixture to achieve the target mini-slump flow. As such, there is a strong indication that elevated dosages of the used PCE may hinder thixotropic development. The ternary mixture with slag and silica fume shows beneficial effects for the short and long term thixotropic development, and reduce the workability loss compared to the reference mixtures and the mixture with slag. Three materials were retained for further analysis: slag, silica fume and attapulgite clay.

4.2 Measurements on concrete

4.2.1 Influence of excess paste layer thickness

Prior to fully developing a VFC mix design suitable for slipform applications, the influence of the excess paste layer thickness was evaluated, in order to understand the contribution of the aggregates and the ratio of packing fraction to maximum packing density. Table 4 shows the mix designs for the evaluated concrete mixtures. The mixture with 40 µm is considered as the reference mixture, while for the mixtures with 30 and 25 µm excess paste layer thickness, two mix designs were created for each: a first series adjusting the dispersant dosage to keep a constant slump flow of around 520 mm, while for the second series, the mass ratio of dispersant to the binder was kept constant. As the purpose of this specific task is to determine the influence of the aggregates, the binder composition is of minor importance. In order to capture as many effects (thixotropy, workability loss, green strength) as possible, a binder combination of 5% silica fume and 95% Portland cement was retained.

Theoretically, the rheological properties should all increase with decreasing excess paste layer thickness, as the volume fraction of aggregates approaches the maximum packing density. However, on paste level, there are two phenomena to take into consideration. First, for equal mixing energy in the concrete, the mixing energy in the paste increases with decreasing excess paste layer thickness, which would likely lead to a (slight) decrease in viscosity of the paste [92]. For the yield stress, the behavior remains unpredictable. When modifying the PCE dosage to keep the slump flow of the concrete constant, the rheology of the paste is altered substantially, especially the dynamic and static yield stresses, which counters the effect of decreasing the excess paste layer thickness.

Table 10 contains all rheological properties of the mixtures. Figure 30 shows the evolution of the dynamic yield stress with varying excess paste layer thickness, both for the initial rheological measurements, as for the measurements with extended time. The mixtures with constant slump flow had a varying PCE dosage, those with constant PCE/binder dosage had varying slump flow. For the mixtures with varying PCE dosage, the yield stress decreases with decreasing excess paste layer thickness at 15 min, indicating that the required

addition of PCE to achieve constant slump flow has a stronger effect on the rheology of the concrete than the increase in aggregate volume fraction (for the evaluated parameters and their range). The mixtures with constant dispersant dosage show a more "logical" trend, although the decrease in yield stress at 30 µm excess paste layer thickness seems less logical (although the more intense mixing energy in the paste may play a role).

Table 10. Rheological properties of mixtures with different excess paste layer thicknesses. Mixtures with extension –SF have constant slump flow, those with –SP have constant SP relative to the binder.

	$\tau_{0,D}$ (PA)	μ_P (PA S)	$\tau_{0,S}$ 1 (PA)	$\tau_{0,S}$ 2 (PA)	$\tau_{0,S}$ 3 (PA)	$\tau_{0,S}$ 4 (PA)	A_{THIX} (PA/MIN)
40-REF	*15'*: 120	*15'*: 28	*15'*: 330	*15'*: 1050	*15'*: 2040	*15'*: 3420	*15'*: 144
	70': 143	*70'*: 24	*70'*: 640	*70'*: 845	*70'*: 2120	*70'*: 3390	*70'*: 93
30-SF	*15'*: 77	*15'*: 41	*15'*: 345	*15'*: 665	*15'*: 1535	*15'*: 2865	*15'*: 71
	70': 205	*70'*: 35	*70'*: 1160	*70'*: 2255	*70'*: 3600	*70'*: 5315	*70'*: 173
25-SF	*15'*: 40	*15'*: 50	*15'*: 240	*15'*: 550	*15'*: 735	*15'*: 1585	*15'*: 49
	70': 91	*70'*: 58	*70'*: 840	*70'*: 1490	*70'*: 2635	*70'*: 4610	*70'*: 134
30-SP	*15'*: 91	*15'*:55	*15'*: 445	*15'*: 1180	*15'*: 1585	*15'*: 3440	*15'*: 114
	70': 429	*70'*: 21	*70'*: 2130	*70'*: 3630	*70'*: 4760	*70'*: 7335	*70'*: 229
25-SP	*15'*: 155	*15'*: 57	*15'*: 815	*15'*: 1480	*15'*: 2775	*15'*: 5225	*15'*: 190
	70': 624	*70'*: 17	*70'*: 2555	*70'*: 4175	*70'*: 5825	*70'*: 7545	*70'*: 251

With elapsed time, the workability loss has an additional effect on the yield stress results. With decreasing excess paste layer thickness, workability loss is expected to be more pronounced, but a strong increase in PCE dosage can completely reverse the workability loss, as demonstrated on the cement pastes. For the mixtures with constant dispersant dosage, the workability loss is substantially larger at lower excess paste layer thickness, resulting in the expected trend for the yield stress data. For the mixtures with constant slump flow, the changes in workability loss due to the excess paste layer thickness and varying PCE dosage are of similar order of magnitude.

Figure 31 shows the results for plastic viscosity, where the results at 15 min follow the expected trend, regardless of whether the dosage of PCE or the slump flow was kept constant. It is known that PCE dosage mainly affects the yield stress of cement-based mixtures, and less the viscosity, explaining why both series of mixtures behave somewhat similarly. However, the mixtures with constant PCE dosage at 70 min show an opposite trend: the viscosity decreases with decreasing excess paste layer thickness. This is expected to be a measurement artefact, as the high yield stress of the mixtures imposes a large domain in the ICAR rheometer to remain stationary, which can lead to an under-estimation of viscosity.

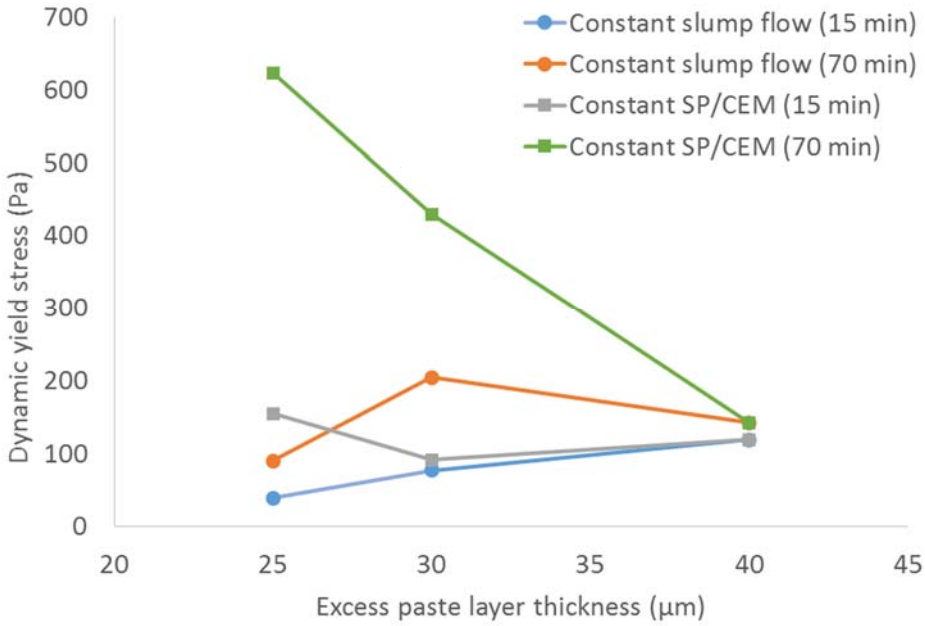

Figure 30. Evolution of dynamic yield stress with varying excess paste layer thickness.

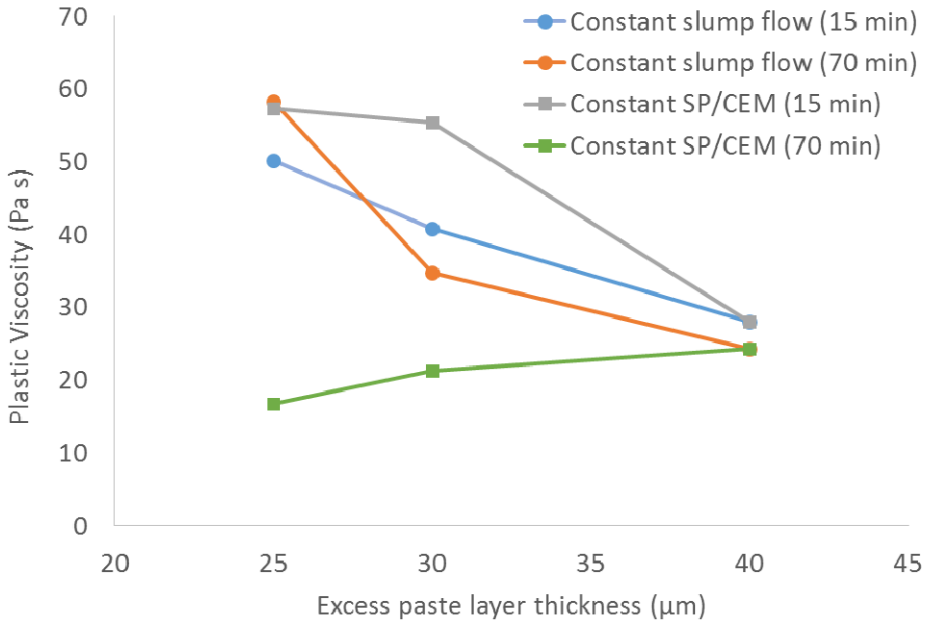

Figure 31. Evolution of plastic viscosity with varying excess paste layer thickness.

Figure 32 shows the values for the static yield stress increase with an elapsed time of 28 minutes (A_{thix}), calculated as the average A_{thix} for intervals 2, 3 and 4, as explained in section 3.5.2. As can be seen, the results in Figure 32 follow closely the results in Figure 30, but the differences seem even more amplified. The mechanisms affecting the yield stress affect the thixotropy in the same manner. Increasing the PCE dosage to achieve a desired workability level has, for the studied mixtures, a more pronounced effect on thixotropy than decreasing the excess paste layer thickness. This goes completely against any logic if the underlying change in cement paste rheology would not be considered. In fact, at 15 min, the best thixotropy result is obtained for a 40 µm excess paste layer thickness. The mixture with 25 µm excess paste layer thickness and constant PCE dosage shows more promising thixotropy, but the slump flow at 15 min is only 360 mm,

seriously compromising its self-consolidating characteristics. Furthermore, the only mixtures resulting in a measurable green strength were the 25 µm excess paste layer mixture with constant SP content, starting at 52 min, and the 30 µm excess paste layer mixture with constant SP content, at 90 and 105 minutes.

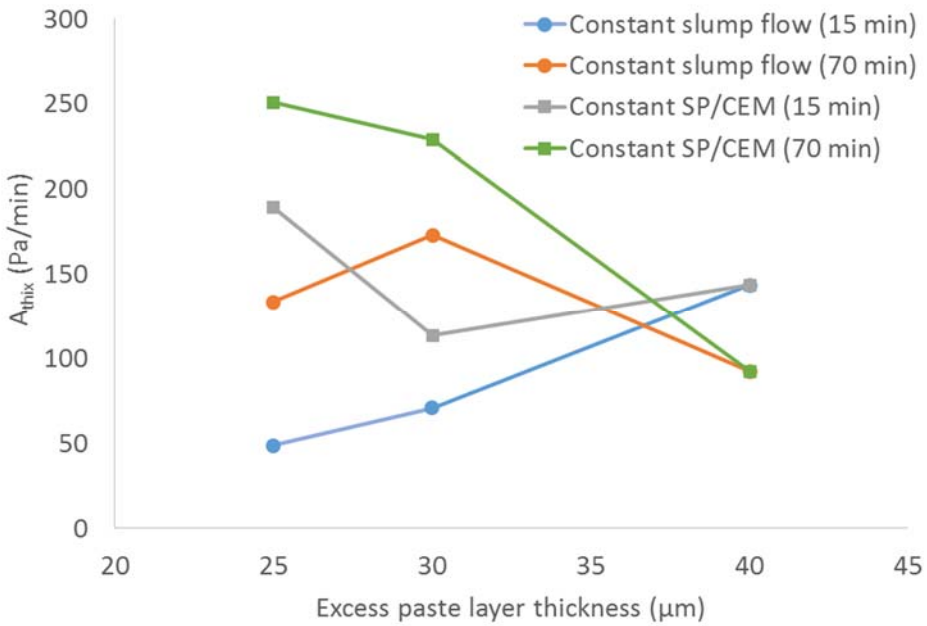

Figure 32. Evolution of thixotropy with varying excess paste layer thickness.

The series of experiments on the excess paste layer thickness have revealed an important aspect: the PCE dosage is crucial in controlling the thixotropy of cement-based materials. This statement is also reflected in the paste results, as the ternary or quaternary paste mixtures with a combination of attapulgite clay and silica fume showed almost no gain in thixotropy, due to their high dispersant contents. Similarly, any mixture with attapulgite clay requires a substantial amount of dispersant. High PCE dosages slow down hydration, which influences the "longer-term" thixotropic development (i.e. the thixotropic development beyond a couple of minutes of rest). Indeed, the paste mixtures with attapulgite clay showed a strong increase in static yield stress immediately after determining the flow curve, but not much yield stress was gained after more extended time. It is believed that the flocculation characteristics of the attapulgite clay cause this immediate increase, but any hydration effect causing a further gain in static yield stress has become negligible due to the PCE dosage. As a consequence, the next task focuses more on finding a mixture with self-consolidating characteristics with the lowest dispersant dosage possible. As minimizing the PCE consumption is the new main goal, the use of VMA and fibers to enhance green strength development was also excluded, as both strategies would require an increase in PCE dosage to achieve equal workability. Based on the cement paste results, mixtures with slag seem more beneficial, and attapulgite clay alone would not be able to provide the long-term green strength development needed.

4.2.2 Optimization of binder composition

From the results of the excess paste layer thickness tests, the 40 µm mixture delivered the best results when adequate slump flow (minimum 500 mm) needed to be obtained. For the remaining mixtures, this excess paste layer thickness was held constant. The binder compositions were altered to mixtures with slag and a combination of slag and attapulgite clay. The binary mixtures (with slag) are expected to show a higher workability loss (based on the cement paste results), making these mixtures more suitable for immediate placement, while a combination of slag and attapulgite clay would be more favorable for extended transportation and remixing on-site. The mix designs of the evaluated mixtures are shown in Table 5, the

results are summarized in Table 11. The mixtures contained 25% slag as SCM from sources A and B. An additional mixture with slag from source B was produced with a slightly reduced PCE content. Quaternary mixtures with attapulgite clay and slag from sources B and C were also evaluated. All mixtures are compared to a binary mixture with silica fume (the reference mixture from section 4.2.1), and one with attapulgite clay.

Table 11. Rheological properties for all mixtures with varying binder composition.

	$\tau_{0,D}$ (PA)	μ_P (PA S)	$\tau_{0,S}$ 1 (PA)	$\tau_{0,S}$ 2 (PA)	$\tau_{0,S}$ 3 (PA)	$\tau_{0,S}$ 4 (PA)	A_{THIX} (PA/MIN)
SL-A	*15'*: 99	*15'*: 32	*15'*: 530	*15'*: 765	*15'*: 1410	*15'*: 2865	*15'*: 83
	70': 461	*70'*: 19	*70'*: 845	*70'*: 1495	*70'*: 2640	*70'*: -	*70'*: 106
SL-B	*15'*: 75	*15'*: 21	*15'*: 270	*15'*: 495	*15'*: 825	*15'*: 1590	*15'*: 53
	70': 278	*70'*: 14	*70'*: 1265	*70'*: 1455	*70'*: 2420	*70'*: 4340	*70'*: 84
SL-B-1	*15'*: 125	*15'*: 44	*15'*: 485	*15'*: 975	*15'*: 1560	*15'*: 3990	*15'*: 114
	70': 558	*70'*: 21	*70'*: 1005	*70'*: 1465	*70'*: 2435	*70'*: 4345	*70'*: 107
AC	*15'*: 124	*15'*: 12	*15'*: 400	*15'*: 820	*15'*: 1710	*15'*: 3415	*15'*: 125
	70': 210	*70'*: 14	*70'*: 820	*70'*: 1495	*70'*: 2645	*70'*: 4410	*70'*: 134
SL-B-AC	*15'*: 79	*15'*: 30	*15'*: 365	*15'*: 940	*15'*: 1945	*15'*: 4025	*15'*: 137
	70': 285	*70'*: 21	*70'*: 835	*70'*: 2130	*70'*: 3690	*70'*: 6495	*70'*: 227
SL-C-AC	*15'*: 68	*15'*: 21	*15'*: 225	*15'*: 510	*15'*: 835	*15'*: 1300	*15'*: 54
	70': 23	*70'*: 25	*70'*: 125	*70'*: 275	*70'*: 620	*70'*: 1415	*70'*: 45

Figure 33 shows the dosage of PCE required for each concrete mixture to achieve the required slump flow of 500 mm. It is worth mentioning though that the slump flow of mixture SL-A was 450 mm, and of SL-B-1 was 550 mm. Mixture SL-B-1 has a slump flow of 500 mm. It is clear that binary mixtures with slag show a lower PCE requirement, while the mixtures with attapulgite clay require a more elevated PCE amount.

Figure 34 shows the change in dynamic yield stress between the 1st and 2nd time the procedure was evaluated, divided by the elapsed time. The mixtures with slag B showed the highest workability loss, while the mixture with slag C and attapulgite clay showed an increase in workability with time. Figure 35 and Figure 36 show the evolution of static yield stresses over the measured intervals, for the 1st and 2nd measurement, respectively. Figure 37 shows the average A_{thix} values derived from those measurements. During the first hour, the binary mixture with slag B, with 550 mm slump flow (SL-B) and the ternary mixture with slag C and attapulgite clay show the lowest thixotropic development, which is probably related to the PCE dosage (SL-B and SL-B-1 are the same mix design, but with slightly different PCE content). The mixtures with silica fume, slag B (with reduced SP content), attapulgite clay, and attapulgite clay with slag B show the better thixotropic development in the first hour, although the development of the stiffness of the silica fume mixture slows down at the end of the first measurement period. The measurements during the second period confirm the slower development for the mixture with silica fume. This mixture is outperformed by all other mixtures, except slag C + AC, during the 2nd hour. In fact, the mixtures with slag A, both mixtures with slag B, and the mixture with attapulgite clay show similar behavior, while the ternary mixture with attapulgite clay and slag B shows the best behavior, despite the more elevated PCE dosages.

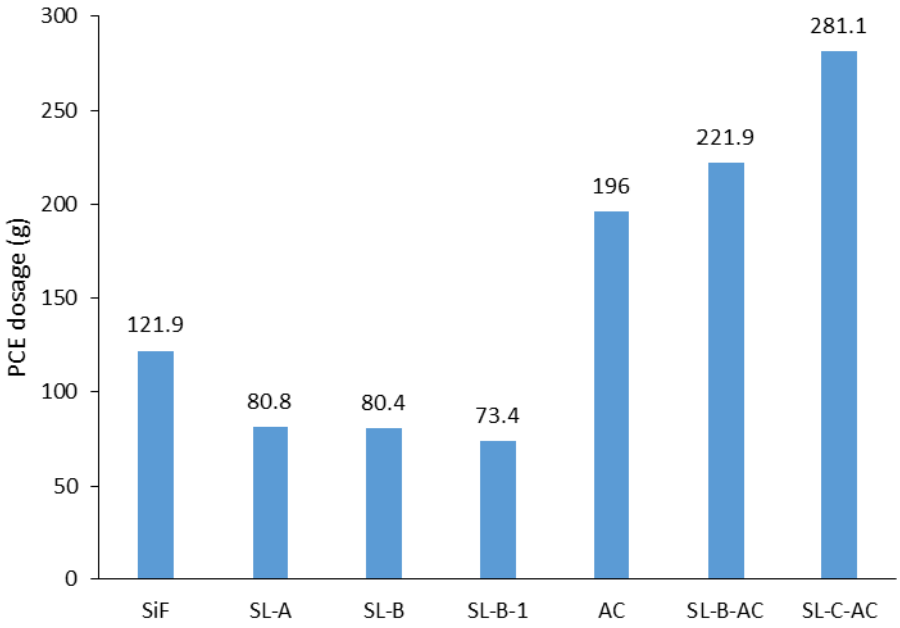

Figure 33. PCE dosage for the evaluated concrete mixtures.

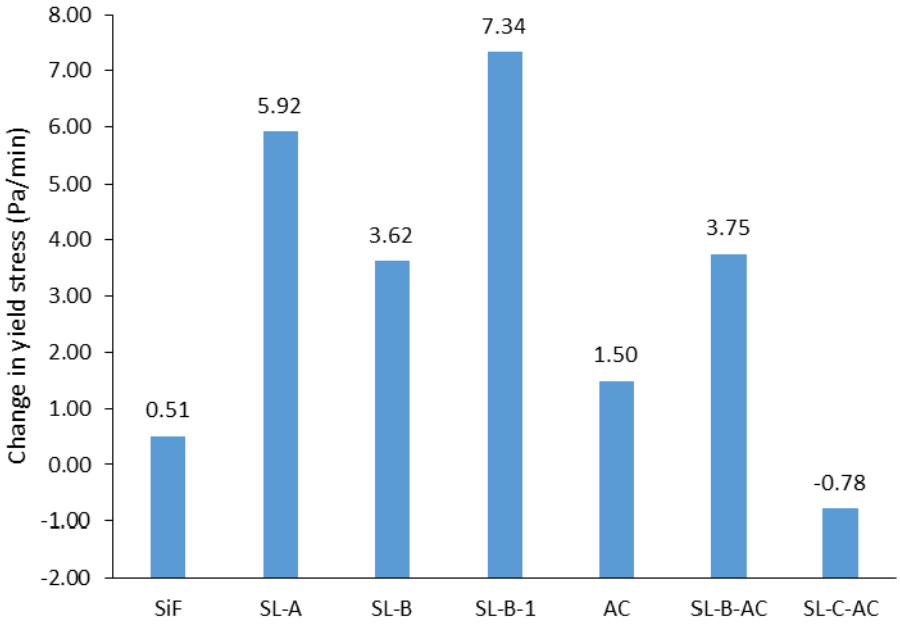

Figure 34. Change in dynamic yield stress for evaluated concrete mixtures.

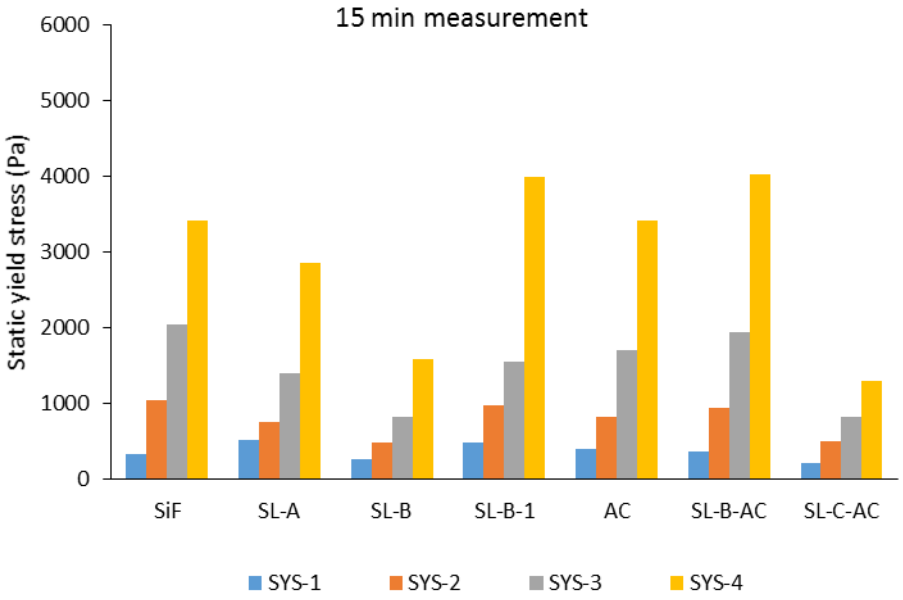

Figure 35. Static yield stress values for the 1st testing series. Each color stands for its respective interval.

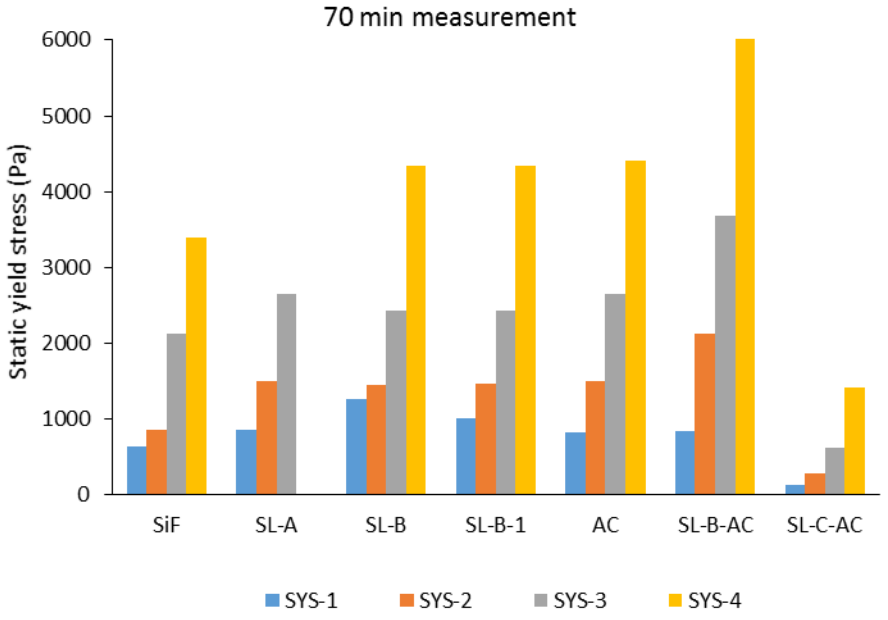

Figure 36. Static yield stress values for evaluated concrete mixtures during the 2nd measurement period, starting at 70 min.

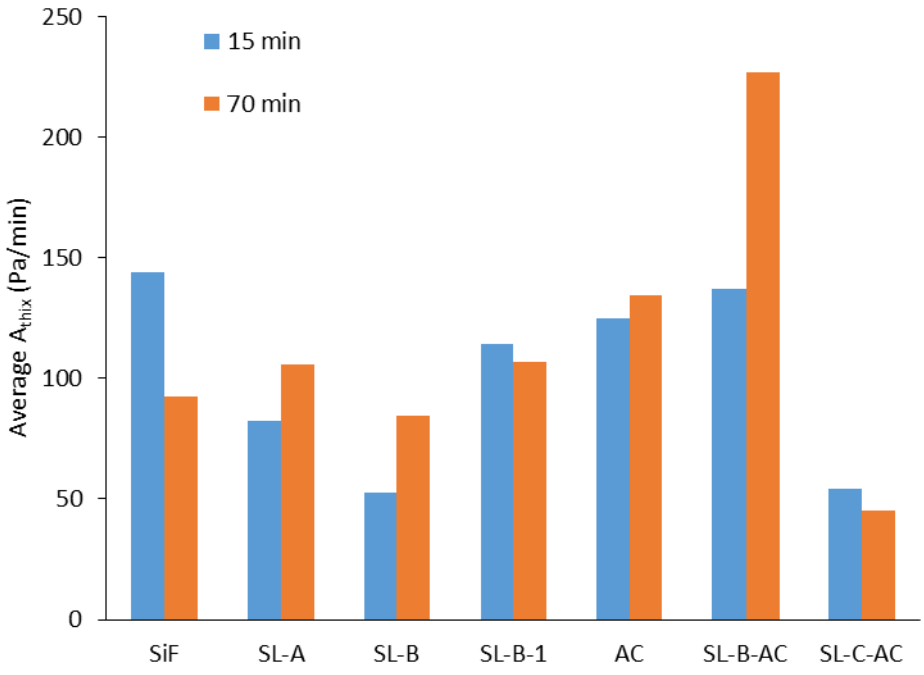

Figure 37. Average gain in static yield stress for the evaluated mixtures.

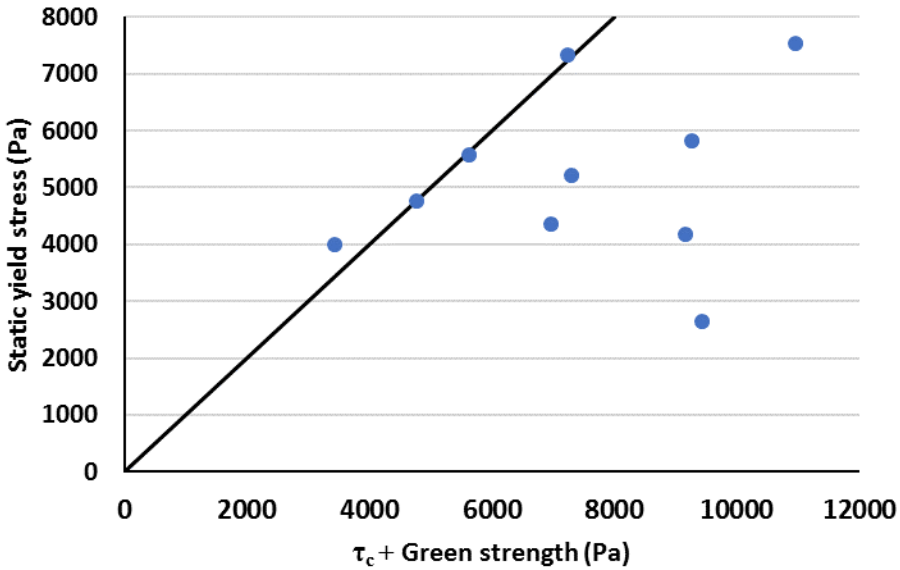

Figure 38. Comparison between measured static yield stress from the ICAR rheometer and the green strength from the cylinder tests.

With this improved thixotropic behavior, more green strength measurement results would be expected. However, the developed green strength method is very sensitive to small movements disturbing the internal structure of the material, and demolding of the fresh cylinders, despite the easy mechanism, was substantially more challenging than anticipated. As such, the number of green strength results is very limited. For the available results, Figure 38 shows a comparison between the static yield stress and the measured green strength. It should be noted that the measured green strength is determined by the stress induced by the self-

weight of the concrete cylinder, according to the von-Mises stress criterion, and the stress induced by the weights added on top of the cylinder until collapse. As such, green strengths below 2718 Pa could not be measured, as this critical value is the minimum for the free concrete cylinder to stand.

The deviation in Figure 38, showing higher green strengths than static yield stress values can be attributed to the repetitive static yield stress measurements in the ICAR rheometer, breaking some of the internal structure at the inner cylinder with each measurement, while the green strength specimens remain undisturbed. However, there are a number of collapsing green strength cylinders, logically not shown in Figure 38, which would be displayed on the left quadrant of the graph. This issue can be attributed to the shortcomings of the green strength test, in particular the demolding of the fresh cylinders.

4.2.3 Summary for concrete testing

The results from the excess paste layer thickness tests revealed an important issue if a constant workability level needs to be achieved: the influence of the PCE dosage is non-negligible, or even dominant in the thixotropic behavior of cement-based materials. Measurements with constant dispersant dosage revealed trends according to expectations based on suspension rheology. As such, the focus shifted to the development of a VFC mixture with reduced PCE content.

Based on the results on the cement paste, different binder combinations were evaluated. As slag from different sources was evaluated, it is clear that the chemical and physical properties play an important role. In the long term, slag is beneficial in the stiffness development, as those mixtures show a more elevated workability loss (compared to the non-slag mixtures). However, the mixture with attapulgite clay and slag C was systematically outperformed by the other mixtures, most likely due to the high PCE demand.

Theoretically, to achieve a self-supporting, self-consolidating concrete mixture, assuming a standard pavement thickness of 150 mm (6 in.), a minimum static yield stress of 2050 Pa is required. With a little safety, assume the requirement is 2500 Pa. None of the mixtures reached 2500 Pa static yield stress before the 3rd static yield stress measurement during the first measuring period. This means that this value is not achieved at a rest time of 15 min, which would induce a slow placement rate, countering the economic argument of this study. There is one mixture which achieves 2500 Pa at 15 min rest time: the mixture with 25 µm excess paste layer for which the dispersant dosage was not adjusted to get self-consolidating characteristics. At later age, simulating a transportation time, remixing on-site and placement, this critical yield stress is achieved quicker (3rd interval, after 16 min of rest), but the slump flow value has dropped below 400 mm for most of the mixtures. Only the binary attapulgite clay and the ternary slag B and attapulgite clay mixtures show a somewhat acceptable slump flow at 70 min: 420, and 430 mm, respectively.

Based on the performed work, it appears that achieving sufficient green strength, while maintaining adequate self-consolidation, without the use of accelerators, is a major challenge, as thixotropic development is strongly hindered by the use of dispersant admixtures. The hard limit to have a minimum slump flow of 500 mm during production, imposed by the research team, seems to be beyond achievable with the materials and strategies employed.

5 Conclusions and Future Research

5.1 Conclusions of this research project

This research project anticipated to further develop vibration-free concrete (VFC) applicable for slipforming applications. A lower limit for the slump flow was set at 500 mm in order to achieve maximum self-consolidation. This value is higher than most reported research on slipform concrete. The research project also intended to develop a mix design for minimal transportation and immediate implementation, and a mix design with low workability loss, intended for remote locations requiring a more extended transportation time. As a result, each measuring procedure was performed shortly after mixing, and with a more extended time.

The research was divided into two parts: a paste component for binder optimization, and a concrete component to investigate the influence of the aggregates and the development of an adequate VFC for slipforming.

For the cement paste study, four parameters were investigated:

- The change in dynamic yield stress: corresponding to the workability loss.
- The change in static yield stress (or stress at very low shear rate), measured immediately after the flow curve, without resting period. This parameter gives an indication on the immediate rebuild of the system.
- The rate of change of static yield stress with elapsed resting time, more commonly known as A_{thix}, mimicking the longer-term (approximately 25 min) structure development.
- The SP consumption to obtain a target mini slump flow, to ensure the obtained results are applicable for the intended workability level.

On cement paste level, the following observations were made:

- A change in w/c in a pure Portland cement paste, followed the expected logic of amplified thixotropy, workability loss and dispersant dosage with decreasing w/c. However, the 0.3 w/c mixture did not gain a substantial increase in thixotropy development compared to the 0.35 w/c mixture.
- The PCE seemed more efficient in maintaining workability, compared to the employed PNS dispersant. The PCE also seemed a bit more efficient in developing stiffness compared to its PNS counterpart at equal w/c.
- Slag, silica fume and attapulgite clay are the SCMs or mineral fillers which showed the most promising behavior for thixotropy development. A major difference between the slag and attapulgite clay mixtures was the low workability retention of the former, while the latter showed almost no workability loss. The attapulgite clay can provide the best immediate rebuild, but shows lower thixotropy development over more extended time.
- Limestone filler, kaolin clay and nanosilica, at the evaluated dosages, were deemed less efficient for the purpose of the project. Metakaolin showed low thixotropy development during the first measurements, but strong development around 1 hour after water-cement contact. The reason for this behavior is currently unknown.
- Combining attapulgite clay and silica fume in the same cement paste mix design, regardless of the presence of slag, requires a substantial amount of dispersant. As a consequence, the workability loss is quasi zero for these mixtures, and the thixotropy development is hindered.
- Combining slag with attapulgite clay appeared to deliver the most promising results.

For the concrete portion of this project, the following parameters were evaluated:

- Change in dynamic yield stress, reflecting workability loss
- Average evolution of the static yield stress, delivering A_{thix}, as a stiffening parameter
- Green strength on freshly cast 100 x 200 mm cylinders

The results on concrete can be divided into two portions: the effect of the aggregates, and final optimization of the mixtures. The effect of aggregates was evaluated through the excess paste layer thickness concept, providing a theoretical framework, applicable to many grain size distributions and aggregate properties. However, the excess paste layer thickness study revealed some surprising results:

- When keeping the dosage of dispersant constant, relative to the binder of the mixture, most rheological properties more or less follow the logical trend: an increase is noted with a decrease in excess paste layer thickness.
- When the dispersant dosage is varied to keep the workability of the concrete constant, the rheology of the paste in the concrete is substantially altered. Especially yield stress values, and by consequence thixotropy values, are largely affected by the increase in PCE dosage with decreasing excess paste layer thickness. In fact, by increasing dosage of PCE (for the evaluated mixtures), the expected beneficial effect of the decrease in excess paste layer thickness is fully countered. Yield stress and thixotropy decrease when reducing the paste content!
- This finding has raised a significant concern, shifting the research to finding a mixture with low dispersant requirements. Selecting the mixtures with low excess paste layer thickness and constant PCE dosage would compromise their self-consolidation, as the slump flow values were below the threshold imposed by the team.

Based on these latter findings, binary and ternary mixtures with slag and attapulgite clay were developed:

- When the mixtures required high dosages of PCE, the thixotropic development was hindered. As such, to develop such mixtures, the dosage of PCE seems the most important parameter of the variables investigated.
- Mixtures with slag, without attapulgite clay, appeared to perform adequately for thixotropy development, but it seems that the rheological properties are sensitive to changes in the slag properties.
- Mixtures with attapulgite clay, and combined attapulgite clay and one of the slag cements appeared to deliver the best results, both in terms of thixotropy and workability retention. However, for a 150 mm layer to be self-supporting, a safe assumption for a minimum static yield stress value would be 2500 Pa. This value can only be reached after considerable waiting time, especially in the first hour after mixing, making the imposed requirement of minimum slump flow of 500 mm and shape stability hard to match, for the evaluated parameters.
- At later age, the mixtures achieve this threshold value for static yield stress after a shorter resting time, but the self-consolidation of those mixtures can be questioned.
- The green strength test delivered some promising results, but the demolding procedure needs to be revised. Small vibrations and concrete sticking to the cylinder walls have led to many premature collapses, despite reaching an adequate static yield stress.
- The best-performing mixture was a concrete with slag (from source B), attapulgite clay, and a 40 µm excess paste layer thickness. However, the thixotropic development was insufficient to provide an economical alternative for slipforming.

5.2 Can a VFC mixture for slipforming with high slump flow be developed?

This research project has shown that enhancing fluidity beyond a certain point and maintaining high thixotropy development cannot be combined with the employed technologies. However, this does not imply that this cannot be achieved, but different materials and procedures are recommended. Since thixotropic development in a longer term is dominated by hydration, controlling this will be essential. If the hydration could be activated at a specified time, or on-demand, slipforming with a self-consolidating concrete would be possible. In fact, all techniques developed for 3-D printing of concrete follow the same physical mechanisms, although high initial fluidity is not required for 3-D printed cement-based materials. Future research will determine which new method would be ideal for slipforming concrete which does not need external consolidation energy

5.3 Outlook on future research

The results have revealed some surprising findings which deserve more attention in the future, reflected in the following questions:

- The interaction of dispersing admixtures with thixotropic behavior:
    - Does the dispersant adsorb on other particles than cement?
    - What in case of silica fume and nanomaterials?
    - Can adsorption be steered, targeted towards a certain material or set of materials?
    - How much does each dispersant affect flocculation? Especially dispersants with steric hindrance are expected to counter flocculation, but to which extent?
    - How much does each dispersant affect hydration? Studies have been performed showing delaying mechanisms, but what is the effect of the dosage, and how can it be quantified?
    - Which effect dominates for thixotropic development? Flocculation or hydration? Understanding this will allow for better tailoring the different components.
- Rheological behavior of cement paste in mortar or concrete. The excess paste layer theory did not fully deliver the anticipated results, even when the composition of the paste was kept constant.
    - It is anticipated that different shear rates in the paste induces minor changes in the rheological properties, which are reflected on larger scale. But how important are those changes? What is their magnitude? Can this be replicated on cement paste scale in rheological experiments?
    - How different is the rheology of cement paste in concrete when mixtures with identical paste and aggregate composition are made, but with different paste volume? Does the paste have a different initial reference state?
    - Can a mechanistic model to include this behavior be built, or does the focus need to shift to the excess water layer concept, taking interaction between dispersants and other chemical admixtures with all powders into consideration?
- Without going in detail in the analysis, the different slag sources showed different rheological behavior. This reveals another important topic for future research:
    - How do the different physical and chemical properties of the different used materials, including cement, exactly influence the rheological behavior?
    - Are the findings dependent on the amount of the material? Does one type of behavior dominate another? Does one material dominate the effect of another?
- The green strength test did not deliver the expected outcome, and the correlation with the static yield stress values is not strong. Some variations need to be incorporated to avoid the shortcomings: vibration-free environments, hydrophobic surface coatings?

6 Acknowledgments

The research team would like to acknowledge the RE-CAST Tier-1 University Transportation Center and the Missouri University of Science and Technology for the financial support of the project. The Center for Infrastructure Engineering Studies (CIES) is acknowledged for making the testing equipment (Anton Paar MCR 302 and the ICAR Rheometer) available to the research team. The technical work of the staff in the Civil, Architectural and Environmental Engineering department: John Bullock and Greg Leckrone, is highly appreciated for the optimization and fabrication of the molds. This project would also not have been possible without the donations of several materials by ActiveMinerals, BASF, Central Plains Cement Company, Lafarge-Holcim, and Lehigh-Hanson. The research team strongly appreciates this support from the industry.

References

[1] American Concrete Pavement Association, "AASHTO/FHWA Industry Joint Training: Construction of Portland Cement Concrete Pavements, NHI Course No. 13133," FHWA HI-96-027, Washington, DC, 1995.

[2] S. Tymkowicz and R. Steffes, "Vibration study for consolidation of Portland cement concrete.," *Transportation Research Record: Journal of the Transportation Research Board,* vol. 1574, pp. 109-115, 1997.

[3] A. Ardani, S. Hussain and R. LaForce, "Evaluation of premature PCC pavement longitudinal cracking in Colorado.," in *Proceedings of the 2003 Mid-Continent Transportation Research Symposium,* , Ames, IA, 2003.

[4] US Army Corps of Engineers, "Engineering and design : evaluation and repair of concrete structures," US Army Corps of Engineers, Washington, DC, 1995.

[5] K. Wang, S. Shah, D. White, J. Gray, T. Voigt, L. Gang, J. Hu, C. Halverson and B. Pekmezci, "Self-Consolidating Concrete--Applications for Slip-Form Paving: Phase I (Feasibility Study) - Federal Highway Administration Transportation Pooled Fund Study TPF-5(098)," Center for Portland Cement Concrete Pavement Technology, Iowa State University, Ames, IA, 2005.

[6] K. Wang, S. Shah, J. Grove, P. Taylor, P. Wiegand, B. Steffes, G. Lomboy, Z. Quanji, L. Gang and N. Tregger, "Self-consolidating concrete, applications for slip-form paving: phase II," National Concrete Pavement Technology Center, Institute for Transportation, Iowa State University, Ames, IA, 2011.

[7] L. Reiter, M. Palacios, T. Wangler and R. Flatt, "Putting concrete to sleep and waking it up with chemical admixtures.," *ACI Special Publication,* vol. 302, pp. 145-154, 2015.

[8] T. Wangler, E. Lloret, L. Reiter, N. Hack, F. Gramazio, M. Kohler, M. Bernhard, B. Dillenburger, J. Buchli, N. Roussel and R. Flatt, "Digital concrete: opportunities and challenges.," *RILEM Technical Letters,* vol. 1, pp. 67-75, 2016.

[9] G. De Schutter, P. Bartos, P. Domone and J. Gibbs, Self-Compacting Concrete, Caithness: Whittles Publishing, 2008.

[10] W. Megid and K. Khayat, "Effect of concrete rheological properties on quality of formed surfaces cast with self-consolidating concrete and superworkable concrete.," *Cement and Concrete Composites,* vol. 93, pp. 75-84, 2018.

[11] B. Pekmezci, T. Voigt, K. Wang and S. Shah, "Low compaction energy concrete for improved slipform casting of concrete pavements.," *ACI Materials Journal,* vol. 104, no. 3, pp. 251-258, 2007.

[12] C. Sotomayor Cruz, Developpement des betons semi autoplacants a rheologie adaptee pour des infrastructures, M.Sc. thesis (in French), Sherbrooke, QC: Universite de Sherbrooke, 2012.

[13] C. Macosko, Rheology Principles, Measurements and Applications, New York: Wiley-VCH, 1994.

[14] J. Yammine, M. Chaouche, M. Guerinet, M. Moranville and N. Roussel, "From ordinary rhelogy concrete to self compacting concrete: A transition between frictional and hydrodynamic interactions.," *Cement and Concrete Research,* vol. 38, no. 7, pp. 890-896, 2008.

[15] N. Roussel, "A thixotropy model for fresh fluid concretes: theory, validation and applications," *Cement and Concrete Research,* vol. 36, no. 10, pp. 1797-1806, 2006.

[16] N. Roussel, "Steady and transient flow behaviour of fresh cement pastes," *Cement and Concrete Research,* vol. 35, no. 9, pp. 1656-1664, 2005.

[17] N. Roussel, G. Ovarlez, S. Garrault and C. Brumaud, "The origins of thixotropy of fresh cement pastes," *Cement and Concrete Research,* vol. 42, no. 1, pp. 148-157, 2012.

[18] G. H. Tattersall and P. F. Banfill, The rheology of fresh concrete, London: Pitman, 1983.

[19] N. Roussel (Ed.), Understanding the rheology of concrete., Oxford: Woodhead Publishing, 2012.

[20] J. Chong, E. Christiansen and A. Baer, "Rheology of concentrated suspensions," *Journal of applied polymer science,* vol. 15, no. 8, pp. 2007-2021, 1971.

[21] D. Feys, R. Verhoeven and G. De Schutter, "Fresh self compacting concrete, a shear thickening material," *Cement and Concrete Research,* vol. 38, no. 7, pp. 920-929, 2008.

[22] D. Feys, R. Verhoeven and G. De Schutter, "Why is fresh self-compacting concrete shear thickening?," *Cement and Concrete Research,* vol. 39, no. 6, pp. 510-523, 2009.

[23] A. Yahia and K. Khayat, "Analytical models for estimating yield stress of high-performance pseudoplastic grout," *Cement and Concrete Research,* vol. 31, no. 5, pp. 731-738, 2001.

[24] J. Mewis and N. Wagner, Colloidal suspension rheology, Cambridge University Press, 2012.

[25] J. Wallevik, Rheology of Particle Suspensions - Fresh Concrete, Mortar and Cement Paste with Various Types of Lignosulfonates. Ph-D dissertation, Trondheim: The Norwegian University of Science and Technology, 2003.

[26] J. Wallevik, "Rheological properties of cement paste: thixotropic behavior and structural breakdown," *Cement and Concrete Reseach,* vol. 39, pp. 14-29, 2009.

[27] H. S. D. Uchikawa and S. Hanehara, "Influence of kind and added timing of organic admixture on the composition, structure and property of fresh cement paste," *Cement and Concrete Research,* vol. 25, no. 2, pp. 353-364, 1995.

[28] D. Bonen and S. Sarkar, "The superplasticizer adsorption capacity of cement pastes, pore solution composition, and parameters affecting flow loss," *Cement and Concrete Research,* vol. 25, no. 7, pp. 1423-1434, 1995.

[29] D. Feys, J. Wallevik, A. Yahia, K. Khayat and O. Wallevik, "Extension of the Reiner–Riwlin equation to determine modified Bingham parameters measured in coaxial cylinders rheometers," *Materials and Structures,* vol. 46, no. 1-2, pp. 289-311, 2013.

[30] M. Geiker, M. Brandl, L. Thrane, D. Bager and O. Wallevik, "The effect of measuring procedure on the apparent rheological properties of self-compacting concrete," *Cement and Concrete Research,* vol. 32, pp. 1791-1795, 2002.

[31] O. Wallevik, D. Feys, J. Wallevik and K. Khayat, "Avoiding inaccurate interpretations of rheological measurements for cement-based materials," *Cement and Concrete Research,* vol. 78, pp. 100-109, 2015.

[32] D. Feys, R. Cepuritis, S. Jacobsen, K. Lesage, E. Secrieru and A. Yahia, "Measuring rheological properties of cement pastes: most common techniques, procedures and challenges," *Rilem Technical Letters,* vol. 2, pp. 129-135, 2018.

[33] R. Phillips, R. Armstrong, R. Brown, A. Graham and J. Abbott, "A constitutive equation for concentrated suspensions that accounts for shear-induced particle migration," *Physics of Fluids A: Fluid Dynamics,* vol. 4, no. 1, pp. 30-40, 1992.

[34] K. Khayat, M. Saric-Coric and F. Liotta, "Influence of thixotropy on stability characteristics of cement grout and concrete," *ACI Materials Journal,* vol. 99, no. 3, pp. 234-241, 2002.

[35] J. Assaad and K. Khayat, "Assessment of thixotropy of self-consolidating concrete and concrete-equivalent-mortar—effect of binder composition and content," *ACI Materials Journal,* vol. 101, no. 5, pp. 400-408, 2004.

[36] J. Assaad and K. Khayat, "Formwork pressure of self-consolidating concrete made with various binder types and contents," *ACI Materials Journal,* vol. 102, no. 4, pp. 215-223, 2005.

[37] J. Assaad and K. Khayat, "Effect of viscosity-enhancing admixtures on formwork pressure and thixotropy of self-consolidating concrete," *ACI Materials Journal,* vol. 103, no. 4, pp. 280-287, 2006.

[38] K. Khayat and J. Assaad, "Use of thixotropy-enhancing agent to reduce formwork pressure exerted by self-consolidating concrete," *ACI Materials Journal,* vol. 105, no. 1, pp. 88-96, 2008.

[39] R. Lapasin, A. Papo and S. Rajgelj, "Flow behavior of fresh cement pastes. A comparison of different rheological instruments and techniques," *Cement and Concrete Research,* vol. 13, no. 3, pp. 349-356, 1983.

[40] R. Ahari, T. Erdem and K. Ramyar, "Thixotropy and structural breakdown properties of self consolidating concrete containing various supplementary cementitious materials," *Cement and Concrete Composites,* vol. 59, pp. 26-37, 2015.

[41] D. Feys, Interactions between rheological properties and pumping of self-compacting concrete, PhD disseration, Ghent: Ghent University, 2009.

[42] H. Barnes, "Thixotropy—a review," *Journal of Non-Newtonian Fluid Mechanics,* vol. 70, no. 1-2, pp. 1-33, 1997.

[43] P. Billberg, Form pressure generated by self-compacting concrete: influence of thixotropy and structural behaviour at rest, PhD dissertation, Stockholm: Royal Institute of Technology, 2006.

[44] P. Banfill and D. Saunders, "On the viscometric examination of cement pastes," *Cement and Concrete Research,* vol. 11, no. 3, pp. 363-370, 1981.

[45] G. Ovarlez and N. Roussel, "A Physical Model for the Prediction of Lateral Stress Exerted by Self-Compacting Concrete on Formwork," *Materials and Structures,* vol. 39, no. 2, pp. 269-279, 2007.

[46] N. Roussel and F. Cussigh, "Distinct-layer casting of SCC: the mechanical consequences of thixotropy," *Cement and Concrete Research,* vol. 38, no. 5, pp. 624-632, 2008.

[47] T. Voigt, J. Mbele, K. Wang and S. Shah, "Using fly ash, clay, and fibers for simultaneous improvement of concrete green strength and consolidatability for slip-form pavement," *Journal of Materials in Civil Engineering,* vol. 22, no. 2, pp. 196-206, 2010.

[48] R. Breitenbücher, D. Sarmiento and F. Holzmann, "Development of Self-compacting Concrete with Good Shape Stability for Slipform Construction," *Advances in Civil Engineering Materials,* vol. 3, no. 2, pp. 104-116, 2015.

[49] H. Hoornahad, E. Koenders and K. Van Breugel, "Towards the development of self-compacting no-slump concrete mixtures," *Journal of Silicate Based Composite Materials,* vol. 3, no. 2, pp. 135-138, 2015.

[50] K. Wang, S. Shah and T. and Voigt, "A novel self-consolidating concrete for slip-form application," *Transportation Research Board,* pp. 1-11, 2006.

[51] I. Topccedil and T. Uygunoğlu, "Influence of mineral additive type on slump-flow and yield stress of self-consolidating mortar," *Scientific Research and Essays,* vol. 5, no. 12, pp. 1492-1500, 2010.

[52] M. Rahman, M. Baluch and M. Malik, "Thixotropic behavior of self compacting concrete with different mineral admixtures," *Construction and Building Materials,* vol. 50, pp. 710-717, 2014.

[53] H. Roby, "Pressure of Concrete on Forms," *Civil Engineering,* vol. 5, 1935.

[54] K. Khayat and J. Assaad, "Effect of w/cm and high-range water-reducing admixture on formwork pressure and thixotropy of self-consolidating concrete," *ACI Materials Journal,* vol. 103, no. 3, pp. 186-193, 2006.

[55] J. Assaad and K. Khayat, "Variations of lateral and pore water pressure of self-consolidating concrete at early age," *ACI Materials Journal,* vol. 101, no. 4, pp. 310-317, 2004.

[56] S. Nunes, P. Oliveira, J. Coutinho and J. Figueiras, "Rheological characterization of SCC mortars and pastes with changes induced by cement delivery," *Cement and Concrete Composites,* vol. 33, no. 1, pp. 103-115, 2011.

[57] K. Juvas, A. Kappi, K. Salo and E. Nordenswan, "The effects of cement variations on concrete workability," *Nordic Concrete Research,* vol. 26, pp. 39-46, 2001.

[58] Z. Quanji, Thixotropic behavior of cement-based materials: effect of clay and cement types. MSc dissertation, Ames, IA: Iowa State University, 2010.

[59] N. Yıldız, M. Erol, B. Baran, Y. Sarıkaya and A. Çalımlı, "Modification of rheology and permeability of Turkish ceramic clays using sodium silicate," *Applied Clay Science,* vol. 13, no. 1, pp. 65-77, 1998.

[60] N. Tregger, M. Pakula and S. Shah, "Influence of clays on the rheology of cement pastes," *Cement and Concrete Research,* vol. 40, no. 3, pp. 384-391, 2010.

[61] R. Ferron, A. Gregori, Z. Sun and S. Shah, "Rheological method to evaluate structural buildup in self-consolidating concrete cement pastes," *ACI Materials Journal,* vol. 104, no. 3, pp. 242-250, 2007.

[62] Z. Quanji, G. Lomboy and K. Wang, "Influence of nano-sized highly purified magnesium alumino silicate clay on thixotropic behavior of fresh cement pastes," *Construction and Building Materials,* vol. 69, pp. 295-300, 2014.

[63] S. Kawashima, J. Kim, D. Corr and S. Shah, "Study of the mechanisms underlying the fresh-state response of cementitious materials modified with nanoclays," *Construction and Building Materials,* vol. 36, pp. 749-757, 2012.

[64] A. Hassan, M. Lachemi and K. Hossain, "Effect of metakaolin on the rheology of self-consolidating concrete," in *Design, production and placement of self-consolidating concrete, pp. 103-112*, Montreal, 2010.

[65] E. Güneyisi and M. Gesoğlu, "Properties of self-compacting mortars with binary and ternary cementitious blends of fly ash and metakaolin," *Materials and Structures,* vol. 41, no. 9, pp. 1519-1531, 2008.

[66] E. Ore and J. Straughan, "Effect of cement hydration on concrete form pressure," *ACI Journal,* vol. 65, no. 2, pp. 111-120, 1968.

[67] K. Khayat, "Viscosity-enhancing admixtures for cement-based materials—an overview," *Cement and Concrete Composites,* vol. 20, no. 2-3, pp. 171-188, 1998.

[68] A. Ghezal, K. Khayat and D. Beaupré, "Effect of High-Range Water-Reducer—Viscosity-Modifying Admixture Combination on Rheological Properties of Concrete Equivalent Mortar," in *Proceedings of the First North American Conference on the Design and Use of Self-Consolidating Concrete (pp. 159-165)*, Stockholm, 2002.

[69] F. Van Der Vurst, S. Grünewald and G. De Schutter, "The impact of VMA on the Rheology, thixotropy and robustness of self-compacting mortars," *Calcined Clays for Sustainable Concrete,* vol. 10, pp. 159-167, 2015.

[70] B. Helnan-Moussa, Y. Vanhove and E. Wirquin, "Thixotropic behaviour and structural breakdown of fresh cement paste: comparison between two types of VMA," *Advances in Cement Research,* vol. 25, no. 4, pp. 235-244, 2013.

[71] J. Khatib, "Performance of self-compacting concrete containing fly ash," *Construction and Building Materials,* vol. 22, no. 9, pp. 1963-1971, 2008.

[72] J. Armaghani, K. Tawfiq, S. Squillacote and M. Bergin, "Accelerated Slab Replacement Using Self-Consolidating Concrete," *Journal of the Transportation Research Board,* vol. 2508, pp. 93-101, 2015.

[73] X. Wang, K. Wang, J. Li, N. Garg and S. Shah, "Properties of self-consolidating concrete containing high-volume supplementary cementitious materials and nano-limestone," *Journal of Sustainable Cement-Based Materials,* vol. 3, no. 3-4, pp. 245-255, 2014.

[74] N. Garg and K. Wang, "Comparing the performance of different commercial clays in fly ash-modified mortars," *Journal of Sustainable Cement-Based Materials,* vol. 1, no. 3, pp. 111-125, 2012.

[75] H. Lindgreen, M. Geiker, H. Krøyer, N. Springer and J. Skibsted, "Microstructure engineering of Portland cement pastes and mortars through addition of ultrafine layer silicates," *Cement and Concrete Composites,* vol. 30, no. 8, pp. 686-699, 2008.

[76] G. Bumanis, D. Bajare and A. Korjakins, "Durability of High Strength Self Compacting Concrete with Metakaolin Containing Waste," *Key Engineering Materials,* vol. 674, pp. 65-70, 2016.

[77] Z. Ge, K. Wang, R. Sun, D. Huang and Y. Hu, "Properties of self-consolidating concrete containing nano-CaCO3," *Journal of Sustainable Cement-Based Materials,* vol. 3, no. 3-4, pp. 191-200, 2014.

[78] S. Kawashima, P. Hou, D. Corr and S. Shah, "Modification of cement-based materials with nanoparticles," *Cement and Concrete Composites,* vol. 36, pp. 8-15, 2013.

[79] J. Han, H. Fang and K. Wang, "Design and control shrinkage behavior of high-strength self-consolidating concrete using shrinkage-reducing admixture and super-absorbent polymer," *Journal of sustainable cement-based materials,* vol. 3, no. 3-4, pp. 192-190, 2014.

[80] I. Krieger and T. Dougherty, "A mechanism for non-Newtonian flow in suspensions of rigid spheres," *Transactions of the Society of Rheology,* vol. 3, no. 1, pp. 137-152, 1959.

[81] F. Mahaut, X. Chateau, P. Coussot and G. Ovarlez, "Yield stress and elastic modulus of suspensions of noncolloidal particles in yield stress fluids," *Journal of Rheology,* vol. 52, no. 1, pp. 287-313, 2008.

[82] BUILD, NT., Compactibility with IC-tester, Espoo: Nordtest, 1994.

[83] F. Mueller, O. Wallevik and K. Khayat, " Linking solid particle packing of Eco-SCC to material performance," *Cement and Concrete Composites,* vol. 54, pp. 117-125, 2014.

[84] K. Khayat and I. Mehdipour, "Design and performance of crack-free environmentally friendly concrete “Crack-Free Eco-Crete”," NUTC, 322, 2014.

[85] M. Geiker, M. Brandl, L. Thrane and L. Nielsen, "On the effect of coarse aggregate fraction and shape on the rheological properties of self-compacting concrete," *Cement, Concrete and Aggregates,* vol. 24, no. 1, pp. 3-6, 2002.

[86] E. Koehler, Aggregates in self-consolidating concrete . PhD dissertation, Austin, TX: The University of Texas at Austin, 2007.

[87] H. Jovein and L. Shen, "Effects of Aggregate Properties on Rheology of Self-Consolidating Concrete," *Advances in Civil Engineering Materials,* vol. 5, no. 1, pp. 235-255, 2016.

[88] C. Kennedy, "The design of concrete mixes," *ACI Journal,* vol. 36, no. 2, pp. 373-400, 1940.

[89] S. Oh, T. Noguchi and F. Tomosawa, "Toward mix design for rheology of self-compacting concrete," in *First International RILEM Symposium on Self-Compacting Concrete (pp. 361-372)*, Stockholm, 1999.

[90] A. Denis, A. Attar, D. Breysse and J. Chauvin, "Effect of coarse aggregate on the workability of sandcrete," *Cement and Concrete Research,* vol. 32, no. 5, pp. 701-706, 2002.

[91] A. Kwan and L. Li, "Combined effects of water film, paste film and mortar film thicknesses on fresh properties of concrete," *Construction and Building Materials,* vol. 50, pp. 598-608, 2014.

[92] D. Feys, G. De Schutter, K. Khayat and R. Verhoeven, "Changes in rheology of self-consolidating concrete induced by pumping," *Materials and Structures,* vol. 49, no. 11, pp. 4657-4677, 2016.